Hybrid Modeling for Estimating Solid Transport Critical Velocity and its Uncertainty

by

Su Meyra Tatar

A thesis submitted to the Graduate Faculty of
Auburn University
in partial fulfillment of the
requirements for the Degree of
Master of Science

Auburn, Alabama
May 9, 2025

Keywords: Solid transport, Hybrid modeling, Semi-mechanistic model, Machine learning

Approved by

Selen Cremaschi, Chair and B. Redd & Susan W. Redd, Eminent Scholar Chair Professor,
Department of Chemical Engineering
Qinghua He, George E. & Dorothy Stafford Uthlaut Endowed Professor,
Department of Chemical Engineering
Chris Kieslich, Assistant Professor, Department of Chemical Engineering

Abstract

The accurate prediction of critical velocity is crucial for multiphase flow applications where the critical velocity is defined as the minimum carrier fluid velocity that transports solid particles without any deposition in wellbores/pipelines. This work uses a parallel structure hybrid modeling approach that combines semi-mechanistic and data-driven models. Three semi-mechanistic models, namely the Mantz (Mantz, 1977), Oroskar and Turian (Oroskar and Turian, 1980), and the Tulsa (Najmi, 2015) models are used as the semi-mechanistic models, and the GPM (Gaussian Process Modeling) (Rasmussen and Williams, 2006) is used as the data-driven model. Using this parallel hybrid modeling structure, two different hybrid modeling frameworks are introduced, which are referred to as 'Hybrid Modeling Framework I' and the 'Hybrid Modeling Framework II'. These frameworks adopt the same parallel hybrid modeling structure and provide prediction uncertainty and aim to make more accurate predictions of uncertainty compared to the semi-mechanistic models. In addition, Hybrid Modeling Framework II includes the development of a semi-mechanistic model selection process to decide which semi-mechanistic model is more appropriate to be used for a given operating condition. Results yield that hybrid models by these two hybrid modeling frameworks provide more accurate predictions of critical velocities compared to the semi-mechanistic models overall based on the root mean square error (RMSE) metric. Additionally, area metric (AM) is used for predictions made by two frameworks which enable us to compare both mean and the variance of the predictions and the measurements. The comparison of the RMSE and AM values for the hybrid models' predictions produced by the two different hybrid modeling frameworks reveals that lower RMSE and AM values are obtained by the Hybrid

Modeling Framework II compared to Hybrid Modeling Framework I. The semi-mechanistic model selection process embedded in Hybrid Modeling Framework II provides more accurate predictions of critical velocity by identifying the correct semi-mechanistic model and the corresponding hybrid model to use for a certain operating condition.

Acknowledgments

I would like to sincerely thank my advisor, Dr. Selen Cremaschi for her support, guidance, and encouragement throughout my studies. I am deeply grateful that I had a chance to work with her and I would like to thank her for guiding me throughout this two and half year's research period with her knowledge, enthusiasm, and patience.

I also would like to thank my thesis committee members Dr. Christopher Kieslich and Dr. Peter He for accepting to be on my thesis committee. Lastly, I thank my family and boyfriend for their love and support throughout this journey. I would like to dedicate my thesis to my brothers and my mother. I am deeply grateful that they have always inspired me and believed in me without any doubt. I cannot express my gratitude enough for their love, support, and patience throughout my life.

Table of Contents

List of Tables

List of Figures

CHAPTER 1 – INTRODUCTION

1.1. Motivation and Background

Solid deposition is one of the main challenges in multiphase flow applications. A common example is in the oil industry, where sand deposition can occur in pipelines during the transport of multiphase fluid from an oil reservoir (Santhamoorthy et al., 2024). The deposited solid particles can lead to both environmental and financial problems (Dabirian et al., 2016). For instance, they may increase operational costs due to potential equipment failures caused by pipeline erosion and corrosion, which, in turn, can result in environmental problems from fluid leakage caused by pipeline corrosion (Dabirian et al., 2016). Additionally, deposited sand can clog pipelines, stopping fluid transport (Obaseki et al., 2022). To prevent this, the fluid must be moved at a high enough velocity to transport the solid particles effectively, allowing them to be separated successfully at a later stage.

There are several models that are used to predict the minimum velocity necessary to transport solids, and they may use different definitions for this velocity. One of these models, the Oroskar and Turian model (Oroskar and Turian, 1980), uses the definition of critical velocity, which this work also adopts. Oroskar and Turian (Oroskar and Turian, 1980) define critical velocity as the velocity at which solid particles are fully suspended from the bottom of the pipeline (Oroskar and Turian, 1980).

The models used for predicting critical velocity can be grouped into three categories: mechanistic, empirical, or semi-mechanistic models, depending on the approaches that were employed in their development (Najmi, 2015). While the mechanistic models are developed using the force balance, the empirical models are developed via curve fitting of experimental data to find the model parameters (von Stosch et al., 2014). The empirical models are purely based on experimental data,

and they typically make valid predictions for the operating conditions within the range of input that the model is built on, and they are not suitable for extrapolation (von Stosch et al., 2014). On the other hand, semi-mechanistic models also depend on the force balance, and the parameters of these models are fine-tuned with the experimental data. Since the parameters of the semi-mechanistic model are fine-tuned with the experimental data, the predictions made by these models are, in general, more aligned with the experimental data compared to the pure mechanistic models (Sansana et al., 2021). However, the critical velocity predictions made by semi-mechanistic models may change significantly for the same operating condition which shows that none of the existing models fully reflect the relevant phenomena. I hypnotize that a hybrid modeling approach that combines knowledge that comes from semi-mechanistic models and information comes from experimental data would yield accurate predictions of critical velocity.

The semi-mechanistic models require detailed knowledge about the system and are based on first principles such as material and energy balances, thermodynamics, transport phenomena, and kinetic laws (Sansana et al., 2021). On the other hand, data-driven models do not require prior knowledge but depend on process data and have poor extrapolation capabilities outside the range of data on which they were built (Bradley et al., 2022). Hybrid models that combine first-principles models and data-driven models, learn from both physics and process data, enabling them to produce more accurate and interpretable results with less data. Additionally, they offer better interpolation and extrapolation capabilities compared to pure mechanistic or data-driven models (von Stosch et al., 2014).

In this thesis, I adopt a hybrid modeling approach to make accurate predictions of critical velocity by combining three semi-mechanistic models, namely Mantz (Mantz, 1977), Oroskar and Turian (Oroskar and Turian, 1980), and the Tulsa models (Najmi, 2015), with a data-driven model,

Gaussian Process Modeling (GPM) (Rasmussen and Williams, 2006). While the semi-mechanistic models are used to predict critical velocity, GPM is employed to predict the model discrepancy and its uncertainty. The model discrepancy is defined as the difference between the experimental measurement of critical velocity and the semi-mechanistic model's estimate of the critical velocity. The Gaussian Process (GP) model, which not only provides predictions but also estimates prediction uncertainty, is chosen as the data-driven model because it is a “powerful nonlinear interpolation tool” (Deng et al., 2022) and is accurate in regression tasks with limited datasets (Rasmussen and Williams, 2006).

1.2. Research Objectives

The research objectives of this work can be summarized as follows.

1- Making accurate predictions of critical velocity and their uncertainty for solid transport in multiphase flow applications.
2- Developing a framework for estimating the critical velocity and its uncertainty for solid transport using hybrid modeling approach.
3- Improving the critical velocity predictions, i.e., predictions with smaller bias and higher precision, using semi-mechanistic selection process.

1.3. Research Activities

The following steps summarize the research activities performed to achieve the research objectives.

1- Calculate the critical velocity for the input conditions of the available experimental data set and assess the performance of the three first principal models, namely Mantz (Mantz, 1977), Oroskar and Turian (Oroskar and Turian, 1980), and the Tulsa models (Najmi,

2015). The data set includes experimentally measured critical velocities for input conditions specified via solid density and solid concentrations, fluid viscosity and densities, and hydraulic and particle diameters.

2- Develop a hybrid modeling approach, which combines the semi-mechanistic models with data-driven models to predict critical velocity for the data set and assess the performance of hybrid models where the GPM (Gaussian Process Modeling) is used as the data-driven model.

3- Perform similarity/dissimilarity analysis of the velocity predictions by semi-mechanistic models to construct data sets where a given semi-mechanistic model provides the best predictions among the models studied.

4- Build a classifier model to determine which model should be used for predicting critical velocity for a given input condition, i.e., a semi-mechanistic selection process. The classifier models are trained with the constructed data sets and employ Random Forest (RF), Support Vector Machines (SVM), and Gaussian Process Classifier (GPC).

5- Develop a hybrid modeling approach that also incorporates the semi-mechanistic model selection process and assess the performance of this hybrid model.

6- Compare the performances of the two hybrid models.

1.4. Significance of the Research

This work aims to predict the velocity necessary to transport solids in multiphase flow applications, i.e., the critical velocity, improve critical velocity predictions, and provide uncertainty estimates for the critical velocity predictions. For this purpose, I assessed (1) the accuracy of three semi-mechanistic models' critical velocity predictions, (2) developed two hybrid modeling frameworks that incorporate data-driven models with the three semi-mechanistic models to improve the critical

velocity predictions and provide uncertainty estimates for the predictions, and (3) analyzed and compared the performance of the two hybrid modeling frameworks. The first hybrid modeling framework employs a GP model in a parallel structure. The second framework adds a semi-mechanistic model selection process in addition to the parallel structure hybrid model.

The semi-mechanistic models that are considered in this study are Mantz (Mantz, 1977), Oroskar and Turian (Oroskar and Turian, 1980), and the Tulsa model (Najmi, 2015). They are chosen because several previous works suggest that these models provide accurate critical velocity predictions (Cremaschi et al., 2013; Soepyan et al., 2012). They are good representative models developed using a variety of development approaches that combine force balances, dimensionless number analysis, and data fitting, yielding empirical and semi-mechanistic models. While the Oroskar and Turian model is a concentration-dependent semi-mechanistic model developed for high solids concentrations (>1000 ppm), the Mantz model is a concentration-independent empirical model that was developed for low concentrations (<100 ppm) of solid particles. The Tulsa model, developed by Kamyar Najmi, PhD, is included in this work as one of the semi-mechanistic models because it has been demonstrated that this model provides accurate critical velocity estimates under various operating conditions using the experimental data set provided by the University of Tulsa (Najmi, 2015).

The analysis of the three semi-mechanistic models revealed that their predictions may differ significantly for the same operating condition and are closer to the critical velocity measurements for certain ranges of input conditions. The difference may be due to the different assumptions used when developing each model and the input data used to estimate their parameters. I hypothesize that the performance of the hybrid model depends on the accuracy of the semi-mechanistic model and that a hybrid model would yield predictions with smaller bias and higher precision if built

using an accurate semi-mechanistic model. To investigate this hypothesis, two hybrid modeling frameworks are developed, referred to as 'Hybrid Modeling Framework I' and 'Hybrid Modeling Framework I.' In Hybrid Modeling Framework I, a parallel structure hybrid modeling approach combines each semi-mechanistic model and a data-driven model, a GP model. In Hybrid Modeling Framework II, a semi-mechanistic model selection process is developed. The process decides which semi-mechanistic and the corresponding hybrid model to use among the three models.

The semi-mechanistic model selection process utilizes classifier models to decide which semi-mechanistic model and the corresponding hybrid model to use to make critical velocity predictions. To train the classifier models, experimental data is labeled using similarity/dissimilarity analysis, which is explained in detail in Chapter 2. The analysis divides available experimental data into two groups for each semi-mechanistic model, with one group including data points for which the semi-mechanistic model provides accurate critical velocity estimates compared to other models and the other group including data points the model does not provide accurate estimates. For example, for the Mantz model, the experimental data set is divided into two groups of data points where the Mantz model has the best performance and the Mantz model doesn't have the best performance compared to the other two semi-mechanistic models. Then, the data points where the Mantz model yielded accurate critical velocity estimates are labeled "Use Mantz model" and the rest are labeled "Do not use Mantz model." The classifier models are trained with these labeled data sets.

The contributions of this work are summarized as:

1) Development of a hybrid modeling approach for making accurate predictions of critical velocity for solid transport and their uncertainty. The hybrid model employs a parallel

structure, Mantz, Oroskar and Turian, and Tulsa models as the semi-mechanistic models, and the GPM as the data-driven model.

2) Development of a semi-mechanistic model selection process to decide which semi-mechanistic model is more appropriate to be used for a given operating condition. The process uses classification models.
3) Introduction of a labeling approach that considers the similarity/dissimilarity of the velocity predictions by the semi-mechanistic models, that labels the experimental data set based on the best predictions provided by a semi-mechanistic model among the models studied.
4) Assessment of the performance of semi-mechanistic models and two different hybrid modeling frameworks.

CHAPTER 2 – METHODOLOGY

2.1. Experimental data

The experimental data set includes 979 data points for the liquid-solid flow (Agudo et al., 2014; Agudo and Wierschem, 2012; Arevalo, 2010; Bohling, 2009; Craven, 1951; Delavan, 2012; Goedde E., 1978; Graf WH et al., 1970; Grass, 1971; Hayden and Stelson, 1971; Hill AL, 2011; IRAJ ZANDI, 1971; Kenchington JM., 1976; Kökpınar and Göğüş, 2001; LOBKOVSKY et al., 2008; Mantz, 1977; Oroskar and Turian, 1980; Patankar et al., 2002; Ramadan et al., 2003; Stevenson and Thorpe, 2002; WHITE, 1970; Wicks, 1971; Zenz, 1964). The data set includes six input variables and experimental measurements of critical velocity. The input variables are solid concentration, solid density, liquid density, liquid viscosity, particle diameter, and hydraulic diameter. The ranges of the experimental data set are given in Table 1. This data set includes a broad range of input variables, notably solid concentration, which significantly impacts critical velocity. Figure 1 includes the histograms for each input variable that shows the distribution of the data set. Figure 1 reveals that despite having wide ranges of input variables, data points don't have even distribution over their range. The input variables other than solid concentration are mostly distributed over the lower values of the provided data range and there are smaller number of data points over the higher values of the provided data range.

Table 1. Ranges and units of the input variables in the experimental data set.

Symbol	Name	Unit	Min	Max
C	Solid concentration/ volume fraction	ppm	1	265000
ρ_l	Liquid density	$\frac{kg}{m^3}$	820	1500
μ_l	Liquid viscosity	$\frac{kg}{m-s}$	0.000378	0.103
ρ_s	Solid density	$\frac{kg}{m^3}$	1040	14950
d_p	Particle diameter	μm	15	5340
D	Hydraulic diameter	m	0.0005	0.44

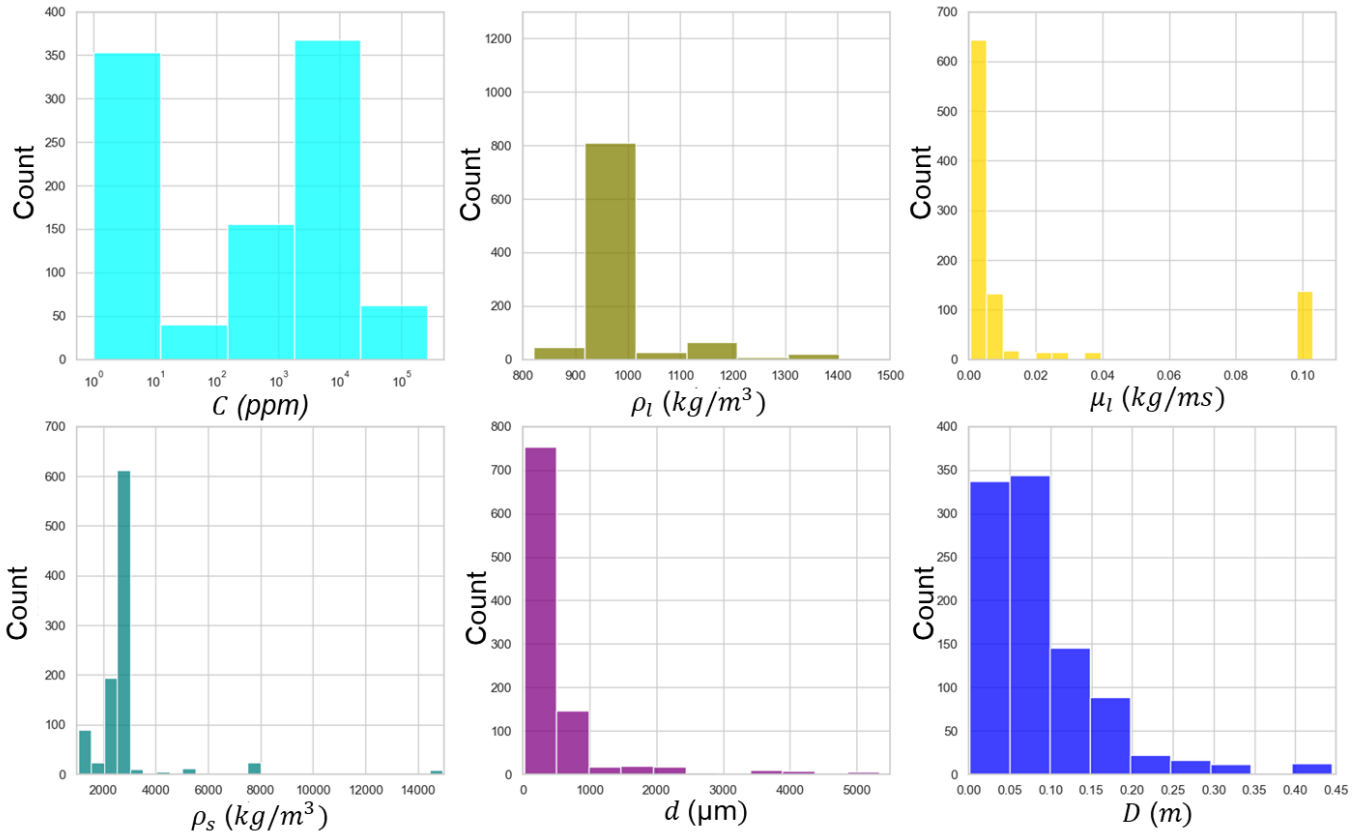

Fig. 1. Histogram of variable values for each input, solid concentration C (ppm), liquid density ρ_l $(\frac{kg}{m^3})$, liquid viscosity μ_l $(\frac{kg}{m-s})$, solid density ρ_s $(\frac{kg}{m^3})$, particle diameter d_p (μm), and hydraulic diameter D (m), in the experimental data for solids transport velocity in liquid-solid flow.

2.2. Hybrid Modeling Framework I

Hybrid Modeling Framework I uses a parallel structure hybrid modeling approach (Fig. 2) (Sansana et al., 2021). In this parallel structure, every semi-mechanistic studied in this work combined with the GP model separately that results in three hybrid sub models. The hybrid model yields critical velocity prediction for an operating condition by combining the estimates of critical velocity by the semi-mechanistic models, y^m, and the estimates of model discrepancy, $\hat{\delta}$, by the GP model.

Eqn. 1 calculates the model discrepancy represented by δ, which is the difference between the experimental measurements of critical velocity and the predictions of critical velocity made by the semi-mechanistic models. In Eqn. 1, the experimental critical velocity measurements are represented by y^e and the critical velocity measurements made by the semi-mechanistic models are represented by y^m. The difference between y^e and y^m is the model discrepancy δ and it is given in Eqn.1.

$$\delta = y^e - y^m \tag{1}$$

The model discrepancy values obtained by Eqn. 1 are used to train the GP model together with the input variables, to obtain model discrepancy estimates, $\hat{\delta}$ and their corresponding uncertainty by the GP model.

In Eqn. (2), the summation of velocity predictions by the semi-mechanistic models, y^m, and model discrepancy estimates by the GP model, $\hat{\delta}$, gives the critical velocity prediction, $\hat{y}^e$, by the hybrid model. The hybrid models yield critical velocity estimates, $\hat{y}^e$, and the corresponding uncertainty which is calculated by the variance from the GP model for 95% confidence interval (CI) (Eqn.3).

$$\hat{y}^e = y^m + \hat{\delta} \tag{2}$$

$$95\%\ CI = \hat{y}^e \mp 1.96\sqrt{Var(\hat{\delta})} \tag{3}$$

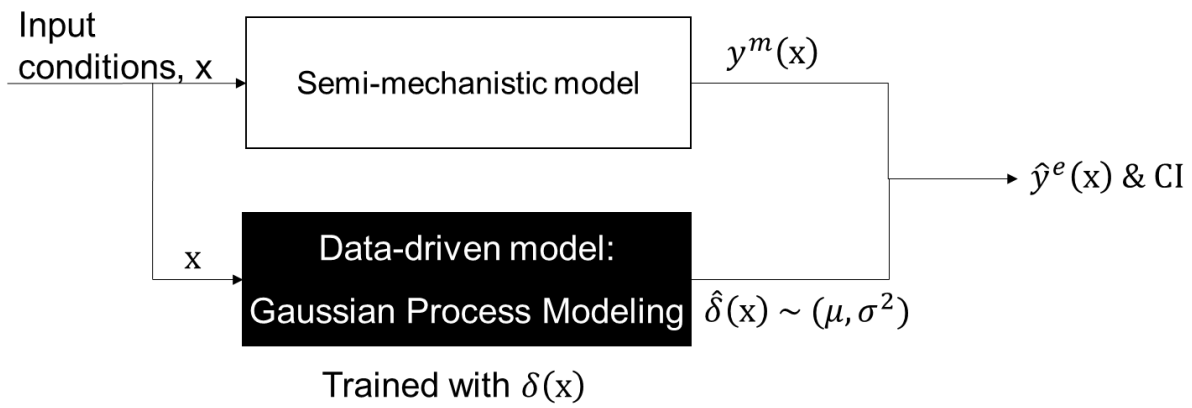

Fig. 2. A parallel structure hybrid modeling approach where X is the input variables, $y^m(x)$ is the semi-mechanistic model predictions of critical velocity, $\delta(x)$ is the model discrepancy, and $\hat{\delta}(x) \sim (\mu, \sigma^2)$ is the model discrepancy estimates by GP model with corresponding mean μ and variance σ^2 , $\hat{y}^e(x)$ & CI is the critical velocity estimates by the hybrid model and the corresponding confidence interval (CI) which is 95% for this work (Deng et al., 2022).

The Hybrid Modeling Framework I includes three different hybrid models by combining three different semi-mechanistic models with the GP models. Specifically, it utilizes the Mantz (Mantz, 1977), Oroskar and Turian (Oroskar and Turian, 1980), and Tulsa models (Najmi, 2015) as the semi-mechanistic models and the GPM (Rasmussen and Williams, 2006) as the data-driven model. The assumptions and the model equation of the semi-mechanistic models are explained in Section 2.2.1, and Section 2.2.2 introduces GPM.

The workflow for Hybrid Modeling Framework I is given in Fig. 3. This workflow is simplified in a way that the parallel structure of hybrid modeling given in Fig. 2 is represented as a box. It shows that Hybrid Modeling Framework I calculates critical velocity and its uncertainty for a given input operating condition. This simplified framework is helpful in comparing Hybrid Modeling

Frameworks I and II, where the simplified workflow for Hybrid Modeling Framework II is given in Fig. 4 in Section 2.3.

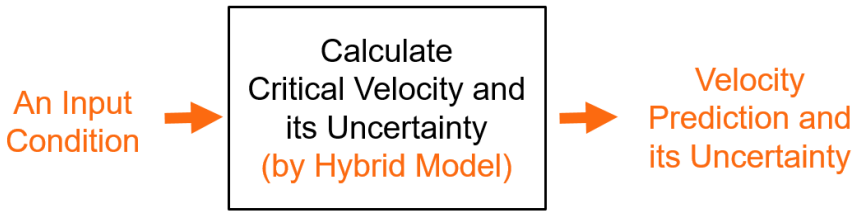

Fig. 3. A simplified workflow for Hybrid Modeling Framework I.

2.2.1. Semi-Mechanistic Solid Transport Models

The Mantz model, Eqn. 4, is an empirical model (Soepyan et al., 2014), which is obtained by fitting a curve to the experimental data (Mantz, 1977). It is developed by assuming that the solid concentration is low (<100 ppm) and for solids transport in horizontal pipes where the carrier fluid is liquid.

$$v_c = 2\left(\frac{D}{d_p}\right)^{0.141}\left(\frac{g d_p^3 \rho_f(\rho_s - \rho_f)}{\mu^2}\right)^{0.495}\frac{\mu}{d_p \rho_f} \tag{4}$$

where the particle Reynolds number and Archimedes numbers are given in Eqns. 5 and 6.

$$N_{Re,\,p} = 2\left(\frac{D}{d_p}\right)^{0.141} N_{Ar}^{0.495} \tag{5}$$

$$N_{Ar} = \frac{g d_p^3 \rho_f(\rho_s - \rho_f)}{\mu^2} \tag{6}$$

The input variables used in Eqns. 4, 5, and 6 are fluid kinematic viscosity (μ), fluid density (ρ_f), solid particle density (ρ_s), gravitational acceleration (g), particle diameter (d_p), and hydraulic

diameter (D). The Mantz Model does not include solid concentration as one of its inputs, and hence, this model ignores the effect of solid concentration on critical velocity.

The Oroskar and Turian model is one of the commonly used models to predict critical velocity for solid transport (Najmi, 2015). This model is based on the balance of the drag forces and turbulence forces of the fluid, and it is developed for the prediction of critical velocity for solid transport at high concentrations (>1000 ppm) in horizontal pipes where the carrier fluid is liquid (Oroskar and Turian, 1980). The model equation (Oroskar and Turian, 1980) is given in Eqn. 7.

$$\frac{v_c}{\sqrt{gd(s-1)}} = 1.85C^{0.1536}(1 - C)^{0.3564}\left(\frac{d}{D}\right)^{-0.378} N_{Re}^{0.09}\left(\frac{2}{\sqrt{\pi}}\left\{\frac{2}{\sqrt{\pi}}\gamma \exp\left(-\frac{4\gamma^2}{\pi}\right) + \int_{\gamma}^{\infty} \exp\left(-\frac{4\gamma^2}{\pi}\right) d\gamma\right\}\right)^{0.30} \tag{7}$$

The γ, v_s, s, N_{Re} terms in Eqn. 7 are defined in Eqns. 8 - 11.

$$\gamma = \frac{v_s}{v_c} \tag{8}$$

$$v_s = \frac{(\rho_s - \rho_l)}{18\mu} g d^2 (1 - C)^2 \tag{9}$$

$$s = \frac{\rho_s}{\rho_l} \tag{10}$$

$$N_{Re} = \frac{D\rho_l\sqrt{gd(s-1)}}{\mu_l} \tag{11}$$

The input variables used in the Eqns. 7 - 11 are particle volume concentration (C), fluid kinematic viscosity (μ), fluid density (ρ_l), solid particle density (ρ_s), gravitational acceleration (g), particle diameter (d_p), and hydraulic diameter (D). Oroskar and Turian Model considers the solid concentration effect on critical velocity in its model equation. Experimental data with wide ranges of solid concentration, fluid densities, and viscosities were used in the development and validation of this concentration-dependent model.

The Tulsa model, which is a concentration-dependent semi-mechanistic model, was developed by Kamyar Najmi as part of his PhD work at The University of Tulsa. It is developed based on a force balance on a single particle grain for carrier fluids of both liquid and gas, where the empirical constants are determined using experimental data (Najmi, 2015). It is shown that this model performs well for a wide range of operating conditions (Najmi, 2015). The Tulsa model for predicting critical velocity is given in Eqn. 12.

$$v_c = \sqrt{\frac{F_\mu}{F_s}} \frac{\left(\frac{1}{9}\right)^{0.5}}{\sqrt{\frac{f}{8}}} \left[d_p g \left(\frac{\rho_p}{\rho_f} - 1 \right) \right]^{0.5} F_c \tag{12}$$

The terms in Eqn. 12 are given in Eqns. 13 to 18.

$$F_s = F_\mu \left[\frac{\pi}{6} d_p^3 g \left(\rho_p - \rho_f \right) \right] \tag{13}$$

$$F_\mu = k(St)^n \tag{14}$$

$$F_c = C_v^{0.1536} (1 - C_v)^{0.3564} \tag{15}$$

$$St = \frac{\rho_p d_p^2 v_c}{18 \mu_f D} \tag{16}$$

$$\frac{1}{\sqrt{f}} = -1.8log\left\{\frac{6.9}{Re_D} + \left[\frac{\left(\frac{d_p}{D}\right)}{3.7}\right]^{1.11}\right\} \tag{17}$$

$$Re_D = \frac{\rho_f v_c D}{\mu_f} \tag{18}$$

The input variables used in Eqns. 12 to 18 are fluid particle volume concentration (C_v), fluid kinematic viscosity (μ_f), friction force (F_s), friction coefficient (F_μ), fluid density (ρ_f), particle density (ρ_p), gravitational acceleration (g), particle diameter (d_p), pipe diameter (D), particle stokes number (St), friction factor (f), and Reynolds number of pipe (Re_D).

2.2.2. Gaussian Process Modeling (GPM)

The Gaussian Process (GP) is a probabilistic supervised machine learning method where it is specified by its mean $m(x)$, and covariance function $k(x, x')$ (Eqn. 19) (Rasmussen, n.d.; Rasmussen and Williams, 2006). Eqn. 19 indicates that "the function *f* is distributed as a GP with mean function *m* and covariance function *k*" (Rasmussen, n.d.). A constant mean and square exponential kernel function is used in this work, which is given in Eqn. 20, where each input has a different length scale l.

$$f \sim \mathcal{GP}(m, k) \tag{19}$$

$$m(x) = a, \text{ and } \mathrm{k}\left(x_p, x_q\right) = \sigma_f^2 \, exp\left(-\sum_{h=1}^{d} \frac{\left(x_p - x_q\right)^2}{2{l_h}^2}\right) + \sigma_n^2 \Delta_{pq} \tag{20}$$

In Eqn. 20, a is the mean function of the GP, *m(x)*, and the kernel function $k\left(x_p, x_q\right)$ is used to compute similarity between two different observations of x_p and x_q (Wang, 2020). In Eqn. 20, the Δ_{pq} represents the Kronecker delta function, which equals to 1 if $p = q$, and l_h represents the

length scale for each input *h,* where d is the dimension of the input x. Additionally, σ_n^2 represents the noise variance and σ_f^2 represents the signal variance, which controls the amplitude of the variations (Ebden, 2015).

The optimal hyperparameters of the GP, $\theta = \{a, \sigma_f, \sigma_n, l_1, l_2, \dots, l_d, \Delta_{pq}\}$, are found via the Maximum Likelihood Estimation (MLE) using the GPy package (De et al., 2017; Rasmussen and Williams, 2006; Wang, 2020). In this work, the GP model is trained to estimate model discrepancy with *k*-fold cross-validation using five folds (Géron, 2023). While the training data set in four folds is used to train the model to find the optimal hyperparameters, one-fold is used as the test set to assess the performance of the trained GP model, and this process is repeated five times using one-fold as the test set each time. Using cross-validation, model discrepancy estimates with their uncertainty are obtained for every data point in the experimental data set.

2.3. Hybrid Modeling Framework II

The Hybrid Modeling Framework II investigates the impact of semi-mechanistic model selection on the accuracy and uncertainty of critical velocity predictions when a parallel structure hybrid model is used. As discussed in Section 3.1, the semi-mechanistic models' performances differ, and some semi-mechanistic models yield critical velocity estimates that are closer to experimental observations compared to others for certain input conditions. I hypothesize that the performance of the hybrid model depends on the accuracy of the semi-mechanistic model and that a hybrid model would yield predictions with smaller bias and higher precision if built using an accurate

semi-mechanistic model. The Hybrid Modeling Framework II enables the test of this hypothesis by combining a semi-mechanistic model selection process with a parallel structure hybrid model.

The simplified workflow for Hybrid Modeling Framework II is given in Fig. 4. Given an input condition, the classifier models select which semi-mechanistic model and corresponding hybrid models should be used. Then, critical velocity and their uncertainty are estimated using the corresponding hybrid model. The details of how each box is built are explained in Sections 2.3.2 and 2.3.3.

Fig. 4. A simplified workflow for Hybrid Modeling Framework II

2.3.1. Preparation of data used in training the classifier models

The semi-mechanistic model selection process embedded in Hybrid Modeling Framework 2 utilizes three different binary classifier models, namely the Mantz model classifier, the Oroskar and Turian model classifier, and the Tulsa model classifier. To train the binary classifier models, the experimental data set is divided into two groups and labeled for each semi-mechanistic model. For example, when the experimental dataset is divided into two groups for the Mantz model classifier, one group of data points is labeled “Use Mantz model,” and the rest of the data points get the label “Do not use Mantz model.” The resulting three labeled data sets have “Use Mantz

model" and "Do not use Mantz model," "Use Oroskar and Turian model" and "Do not use Oroskar and Turian model," and "Use Tulsa model" and "Do not use Tulsa model" labels.

Comparison and analysis of the three semi-mechanistic models for the experimental data set revealed that the predictions of two of the models are quite similar for some input conditions (Section 3.1). Therefore, prior to labeling studies, the Bland-Altman (BA) plots (Altman and Bland, 1983) are employed to assess whether the predictions of the models were similar or not for each input condition. We note that the Bland-Altman (BA) plots are not used to determine whether the predictions are accurate or not, only that they are similar or dissimilar to one another.

The Bland-Altman (BA) plots are used in agreement analysis to compare two measurement methods i.e., method A and method B (Altman and Bland, 1983). The x-axis of BA plots usually shows the mean values of every measurement made by two different methods, and the y-axis plots the difference between these measurements. The BA plot quantifies the agreement between methods A and B using the mean and variance of the differences or the percent difference between these measurements of the two methods (Giavarina, 2015). The mean value of differences on y-axis is a metric that quantifies how much the two methods differ on average. As the two measurement methods, on average, yield similar measurements, the mean value of differences would get closer to zero. The difference between the mean value of differences and the zero line is considered biased (Altman and Bland, 1983; Giavarina, 2015). Additionally, while looking at the variance of the distribution on the y-axis, which is basically the difference or the percent difference of these measurements, one can determine an agreement limit. For example, based on the distribution of the difference between two methods, the agreement limit could be determined to be in 95% confidence intervals (CI) which correspond to the +1.96 std (standard deviation) and -1.96 std. The data points within the range of agreement limits are in agreement for the two

different methods. However, this method of BA plots does not suggest any confidence interval limit for any case. This is something that needs to be determined by the specific area that it will be used for (Giavarina, 2015).

An example of a BA plot is given in Fig. 5. This is one of the BA plots that we used to compare the critical velocity predictions by two semi-mechanistic models (Section 3.3.1). For our analysis, we utilized the volumetric sand concentration as the x-axis. The y-axis for the BA plot is the modified percent differences between the Oroskar and Turian and Tulsa model predictions.

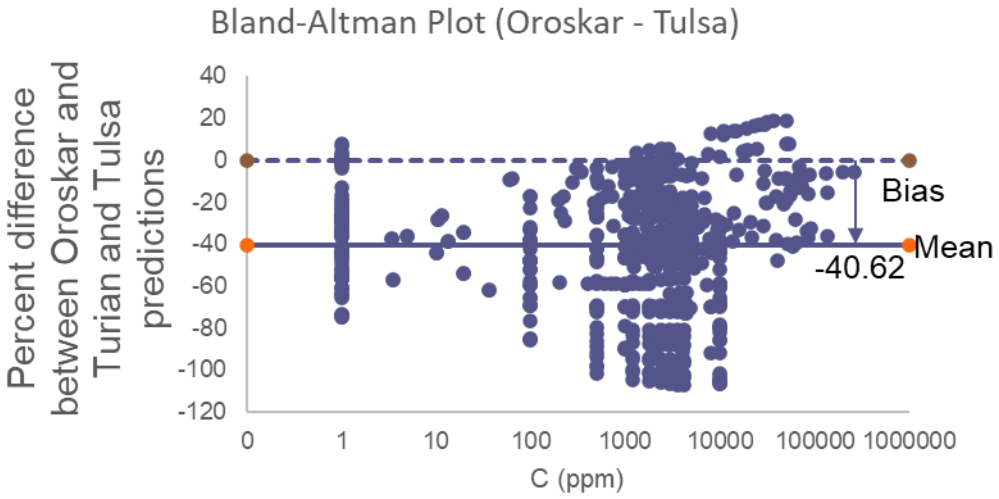

Fig. 5. An Example Bland-Altman Plot

This work uses BA plots to answer the question of whether the predictions made by the three semi-mechanistic models are similar or dissimilar without looking at whether these predictions are accurate or not.

Modified percent differences, which are given in Eqns. 21 to 23, are used for the y-axis of the BA plots of the pairwise comparisons of the semi-mechanistic models' critical velocity predictions where the variables y^m_{Mantz}, $y^m_{Oroskar}$, and y^m_{Tulsa}corresponds to the velocity predictions made by

the Mantz, Oroskar and Turian, and Tulsa models respectively. The BA plots are analyzed to determine the bias and set the agreement limit between the models in pairs. The resulting BA plots and the corresponding agreement limits based on Eqns. 21-23 are discussed in Section 3.3.1.

$$percent\ difference^{\%}_{M\ \&\ OT} = \frac{(y^m_{Mantz} - y^m_{Oroskar})}{\frac{y^m_{Oroskar} + y^m_{Manzt} + y^m_{Tulsa}}{3}} * 100 \quad (21)$$

$$percent\ difference^{\%}_{OT\ \&\ T} = \frac{(y^m_{Oroskar} - y^m_{Tulsa})}{\frac{y^m_{Oroskar} + y^m_{Manzt} + y^m_{Tulsa}}{3}} * 100 \quad (22)$$

$$percent\ difference^{\%}_{M\ \&\ T} = \frac{(y^m_{Mantz} - y^m_{Tulsa})}{\frac{y^m_{Oroskar} + y^m_{Manzt} + y^m_{Tulsa}}{3}} * 100 \quad (23)$$

The experimental data set is divided into four groups using the agreement limits (Section 3.3.1). These groups are: 1) the Oroskar and Turian model and the Tulsa model are similar (O&T – T similar in Fig. 6), 2) the Mantz model and Oroskar and Turian model are similar (M – O&T similar in Fig.6), 3) the Mantz model and Tulsa model are similar (M – T similar in Fig.6), and 4) dissimilar (Dissimilar in Fig.6). The data points in each group are further divided based on which model(s) predictions had the smallest bias. For example, as can also be seen in Fig. 6, the data points that have similar predictions by the Oroskar and Turian and Tulsa models (O&T – T similar in Fig. 6) are divided into two subgroups, i.e., the "Mantz model is the best" or "Oroskar and Turian and Tulsa models are the best". Due to the underlying assumption that the predictions made by Oroskar and Turian and Tulsa models are similar in the O&T – T similar group, the data points that are in

the “Oroskar and Turian and Tulsa models are the best” group are labeled with “Use Oroskar and Turian model” and “Use Tulsa model”.

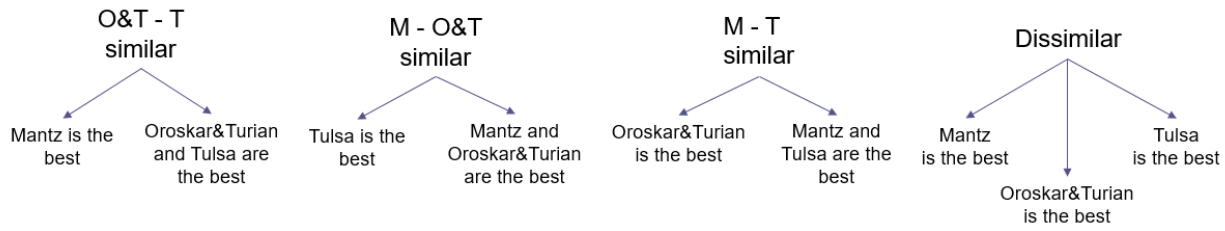

Fig 6. Grouping the similar/dissimilar data sets as the best predictions.

Each data group is divided into subgroups, as shown in Fig. 6, and data points in each sub-group are labeled using a similar approach. All data points in the “Mantz model is best” subgroup are labeled “Use Mantz model,” and the remaining data points are labeled “Do not use Mantz model.” Similar binary labels are added to each data point for the Oroskar and Turian model and Tulsa model, respectively. The resulting labels for each semi-mechanistic model are discussed in Section. 3.3.1.

2.3.2. Selection of semi-mechanistic models using classifiers

This section provides the process developed to select semi-mechanistic models, which corresponds to the first box in the simplified workflow of Hybrid Modeling Framework II in Fig. 4. The process uses binary classifier models to decide which semi-mechanistic model to use, and it uses the labeled data sets to train the classifier models. Fig. 7 outlines how the classifier models are trained. For example, Mantz Model Classifier is trained using the data sets labeled “Use Mantz model” and “Do not use Mantz model” (Fig. 7). Three classifier modeling approaches, Random Forest (RF), Support Vector Machines (SVM), and Gaussian Model Classifier (GPC), are tested for

training the binary classifiers. Three classifier models are trained for each semi-mechanical model yielding nine classifier models in total. The performances of these classifier models for every semi-mechanistic model are discussed in Section 3.2. A brief introduction to the RF, SVM, and GPC models are included next.

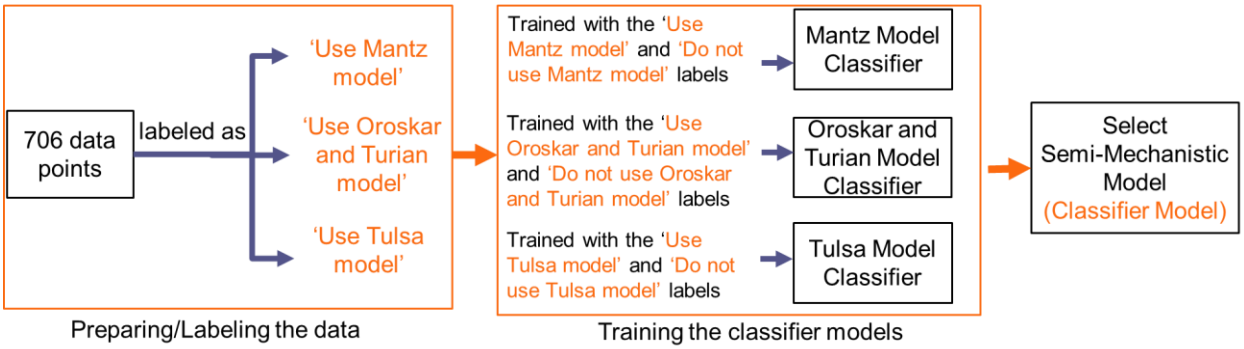

Fig. 7. Building of semi-mechanistic model selection process by classifier models.

Random Forest Models

Random forest is an ensemble learning method that combines the outcomes of multiple decision trees, which are constructed based on a randomly generated subset of features (inputs) (Breiman, 2001). This decision tree method aims to split the feature space into simpler regions to construct a tree-based structure (James et al., 2023). Random forest is the extension of bagging, bootstrap aggregating, which is another ensemble learning method, and it provides improvement over bagging while introducing random feature selection in splitting the trees each time. It means only a randomly selected subset of features is considered in splitting the trees instead of all feature set. The output of the Random Forest is a class that gets the majority votes from the decision trees for the binary classification tasks (James et al., 2023).

The RF model hyperparameters considered in this study are the number of trees and the maximum number of features considered for each split in the decision trees. The optimal hyperparameters

are found using a grid search strategy with cross-validation with five folds (Géron, 2023). First, the data set is divided into two groups: the training and the test sets. For the training set, the model is trained with four folds and validated for one-fold for one set of combinations of the hyperparameters. This procedure is repeated five times. The F1 Score (an evaluation metric discussed in Section 2.4.1) values are averaged for five folds. The optimal hyperparameters are the ones that give the highest average F1 Score. The model is trained with the whole training set using the optimal hyperparameters, and the performance of this model is assessed on the test data set.

Support Vector Machines

Support Vector Machines (SVM) are one of the commonly used machine learning algorithms for classification tasks and it is a supervised machine learning algorithm that classifies the data by finding the optimal line or hyperplane between different classes (Géron, 2023). This work uses the 'C', 'gamma', and different 'kernels' as the hyperparameters of the SVM. The parameter 'C' corresponds to the margin between the hyperplanes and the lower values of parameter C corresponds to a larger margin between the planes. On the other hand, the parameter 'gamma' determines how wide the decision boundary will be. While the smaller value of gamma corresponds to a wider decision boundary, the larger value of gamma corresponds to a narrower decision boundary. The optimal hyperparameters for the SVM are found through the same grid search strategy with cross-validation, which is explained in the Random Forest section.

Gaussian Process Classifier

The details for GP (Gaussian Process) modeling are given in Section 2.2.2. The GPC (Gaussian Process Classifier) which implements GP, is one of the machine learning algorithms used for the classification tasks that produces class probabilities of the labels (Rasmussen and Williams, 2006). This work uses the GPy package to build the GPC model (De et al., 2017). Different kernels

are used as hyperparameters and the optimal hyperparameters are found through the same grid search strategy with cross-validation, which is explained in the Random Forest section.

2.3.3. Calculation of critical velocity and its uncertainty with hybrid models

This section corresponds to the second box in the simplified workflow of Hybrid Modeling Framework II in Fig. 4, which is the calculation of critical velocity and its uncertainty by the hybrid models. Fig. 8 below shows how these hybrid models are built. For this part, the parallel hybrid models' structure is the same as Hybrid Modeling Framework I, in Section 2.2, Fig. 2. However, in Hybrid Modeling Framework I, the GPM models are trained with the model discrepancy values for the whole data set (706 data points) by a certain semi-mechanistic model. Here, in this framework, the GPM models are trained with the labeled data set. For example, hybrid models in this framework include semi-mechanistic models and GPM models in the hybrid model structure. The GPM model that is used with the Mantz model is trained with the model discrepancy values of "Use Mantz model" labeled data points. With that, the corresponding GPM models are trained with model discrepancy values of 98 data points by the Mantz model, 355 data points by the Oroskar and Turian model, and 524 data points by the Tulsa models respectively. These GPM models are used with the corresponding semi-mechanistic models in the Hybrid Modeling Framework II.

For unseen data, this Hybrid Modeling Framework II starts with the selection of a semi-mechanistic model. Once it is decided which semi-mechanistic model to use, then the critical velocity predictions and their uncertainty can be calculated with the corresponding hybrid model where its GPM model is trained with the labeled data set. Here, it should be noted that we ask the question of which model to use for three different classifier models. It means that we might be suggested to use multiple models or none of the models at the same time for an unseen operating

condition.

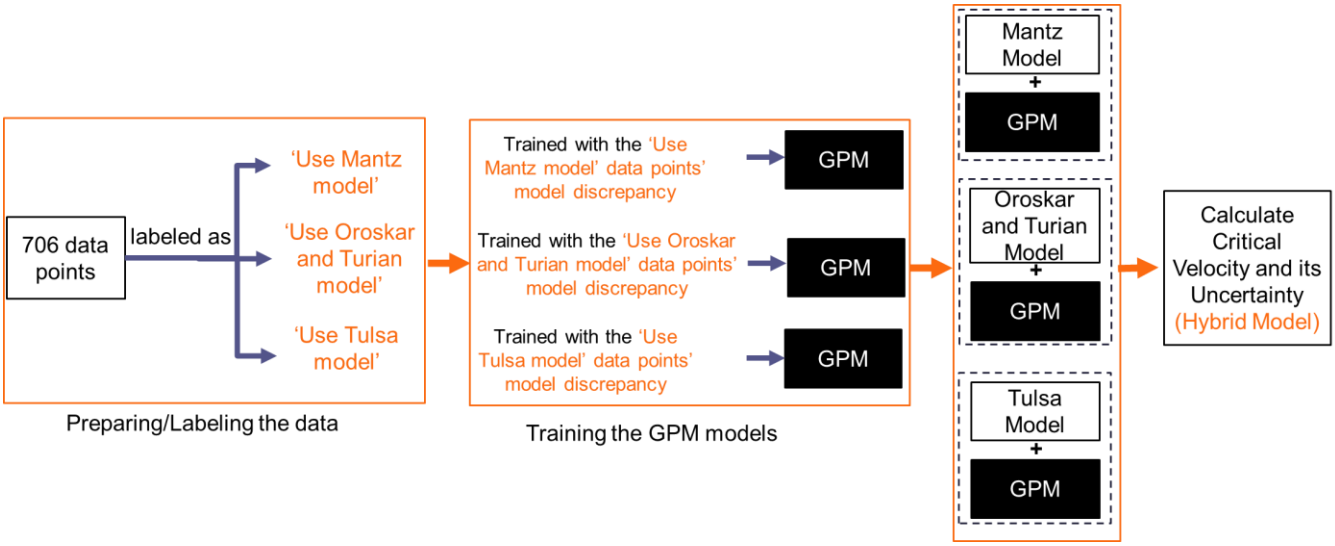

Fig. 8. Building of hybrid models using labeled data.

2.4. Evaluation metrics

2.4.1. Evaluation metric used for the classifier models

The evaluation metrics that are used to assess the performance of the classifier models are confusion matrix, recall, precision, F1 score, MCC, and AUC.

Confusion matrix

Confusion matrix produces 2x2 matrix for a binary classifier that shows, True Positives (TP), True Negatives (TN), False Positives (FP), and False Negatives (FN). A representative confusion matrix is given in Fig. 9. While the TPs and represents the correctly predicted labels of 1, FPs represents the labels that are falsely predicted as 1. Also, TNs and represents the correctly predicted labels of 0, FNs represents the labels that are falsely predicted as 0.

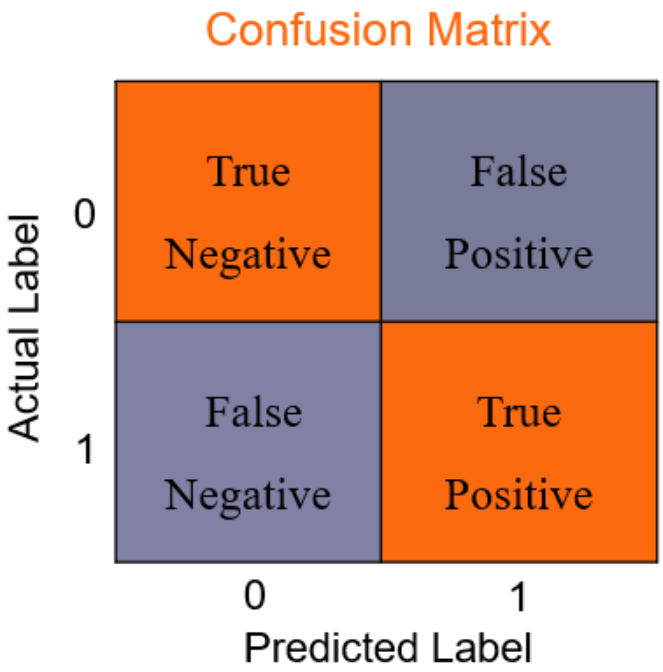

Fig. 9. A representative confusion matrix.

Accuracy

Eqn. 24 shows the definition of accuracy. It is basically the ratio of the number of correct predictions to the total number of predictions. This might be a misleading metric in the case of dealing with imbalanced data sets.

$$Accuracy = \frac{(TP + TN)}{(TP + FP + TN + FN)} \tag{24}$$

Precision

Precision formula is given in Eqn. 25. This metric shows the ratio of correctly predicted labels to the number of labels that are predicted as positive.

$$Precision = \frac{(TP)}{(T) + (FP)} \tag{25}$$

Recall

Recall is formulated as follows in Eqn. 26. It shows the number of labels that are correctly predicted by the model out of the actual labels.

$$Recall = \frac{(TP)}{(TP) + (FN)} \tag{26}$$

F1 Score

This is an effective metric because it combines precision and recall. The corresponding equation for F1 Score is given in Eqn. 27. It is the harmonic mean of precision and recall and the maximum value of F1 Score can be obtained when precision and recall are equal to each other. The F1 Score is expected to be in [0-1] range.

$$F1\ Score = \frac{2\ * Precision\ * Recall}{Precision + Recall} \tag{27}$$

MCC (Matthews correlation coefficient) Score

MCC score another efficient metric that is used given in Eqn. 28. It considers all the elements in the confusion matrix and a good MCC score can be obtained if the model predictions are good considering every item on the confusion matrix. The MCC score is expected to be between -1 and 1 where the 1 corresponds to an excellent classifier and -1 corresponds to an inverse prediction. Additionally, 0 MCC score means that classifier makes a random prediction. The MCC score is a good evaluation metric even in the case of having imbalanced data set.

$$MCC = \frac{TP * TN - FP * FN}{\sqrt{(TP + FP) * (TP + FN) * (TN + FP) * (TN + FN)}} \quad (28)$$

2.4.2. Evaluation metrics used for the GPM model

To assess the performance of the GPM models and the corresponding hybrid models' performances three different evaluation metrics, namely the RMSE, AM, and CS are used.

Area Metric

An example Area Metric (AM) representation is given in Fig.11. Area metric corresponds to the shaded area between the cumulative probability distributions of $\hat{y}^e$ and y^e where the $\hat{y}^e$ value represents the velocity prediction by the hybrid model and the y^e represents the experimental measurements of the velocity. Smaller values of shaded area represent lower values of AM which indicates more accurate predictions of critical velocity.

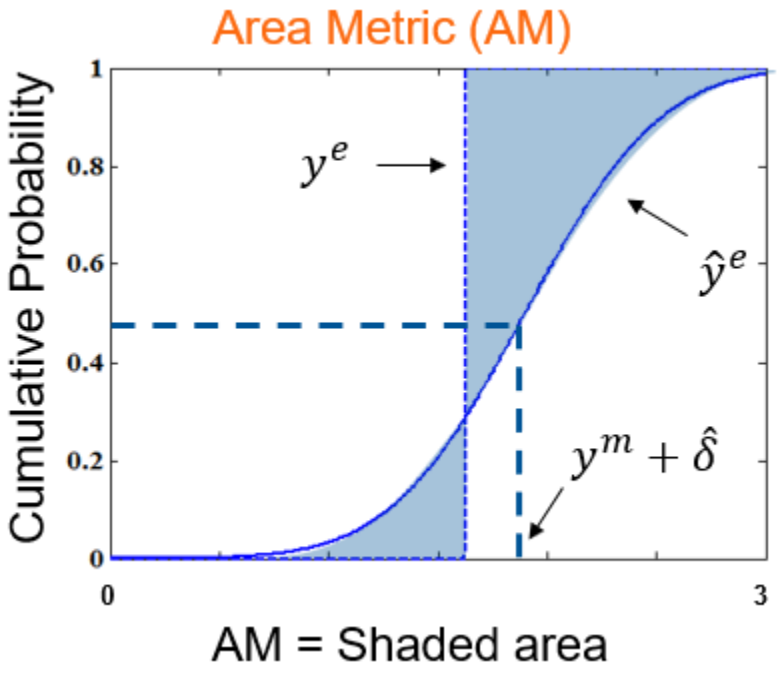

Fig. 10. An example AM (Area Metric) representation.

RMSE (Root Mean Square Error)

The RMSE formula is given in Eqn. 29 where the $\hat{y}^e$ value represents the velocity predictions by the hybrid model and the y^e represents the experimental measurements of the velocity and N corresponds to the total number of predicted data points. The RMSE metric is used to measure the average difference between the model predictions and the corresponding actual values.

$$RMSE = \sqrt{\frac{1}{N}\sum_{i=1}^{N}\left\|y_{(i)}^{e} - \hat{y}_{(i)}^{e}\right\|^2} \tag{29}$$

Calibration Score

Calibration Score (CS) corresponds to the percentage of number of experimental measurements that are covered by a certain amount of predicted confidence interval. The CS corresponds to the percentage of number of experimental measurements of critical velocity that are covered by certain confidence interval which is by 95% in this work.

$$\% = \frac{number\ of\ points\ covered\ by\ predicted\ 95\%\ confidence\ interval}{total\ number\ of\ points} \tag{30}$$

CHAPTER 3 – RESULTS AND DISCUSSION

3.1. Performance of the Semi-Mechanistic Models

Critical velocity predictions made by the three semi-mechanical models can be found in Fig. 11. In Fig. 11, the y^m values on the y-axis represent the critical velocity predictions made by the semi-mechanistic models, the y^e values on the x-axis represent experimental critical velocity measurements for these data points. The blue line on these figures is the parity line. The RMSE values for the predictions are 0.876, 0.491, and 0.475 for the Mantz, Oroskar and Turian, and Tulsa models, respectively. The RMSE for the Tulsa model is the lowest among semi-mechanistic models. It is noted that Mantz, Oroskar and Turian, and Tulsa models yielded predictions for 979, 910, and 775 data points, respectively. We were not able to generate predictions for all data points using the Oroskar and Turian, and Tulsa models due to numerical solution issues.

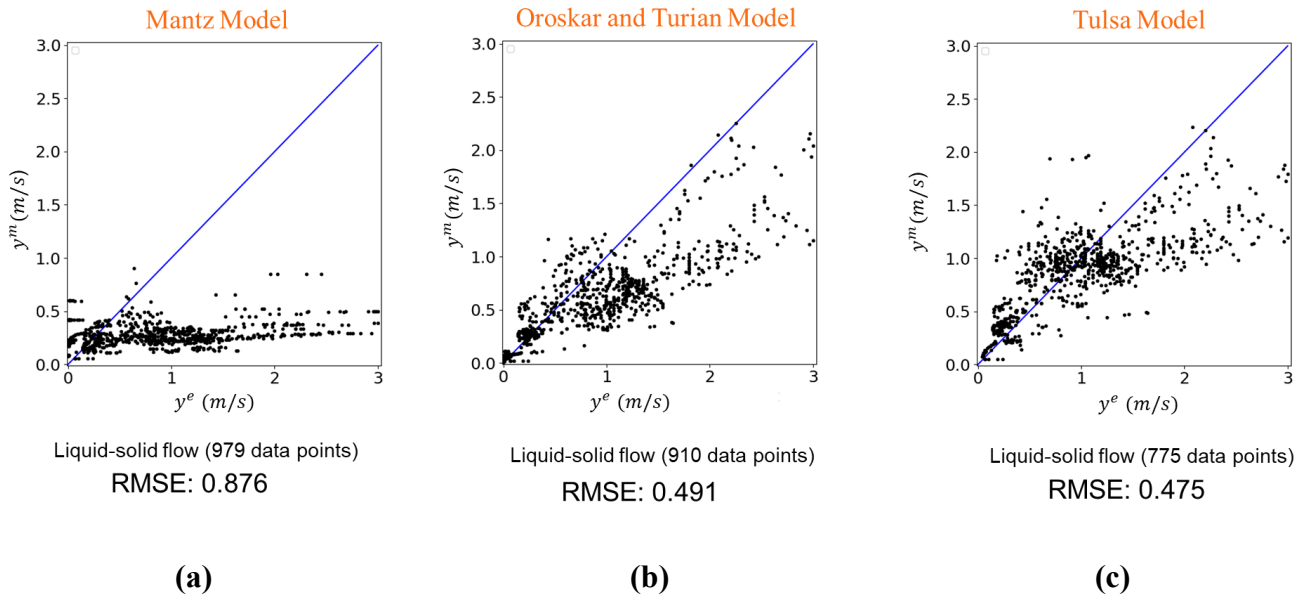

Fig. 11. Critical velocity predictions by three semi-mechanistic models.

To reduce the potential bias that may be introduced due to missing predictions, we will continue our analysis using the 706 data points for which all semi-mechanistic models provided critical velocity predictions. These predictions are plotted against the experimental observations in Fig. 12. The RMSE values for these predictions are 0.99, 0.58, and 0.48 for the Mantz, Oroskar and Turian, and Tulsa models, respectively. Similarly, the RMSE for the Tulsa model is the lowest RMSE among semi-mechanistic models for these 706 data points.

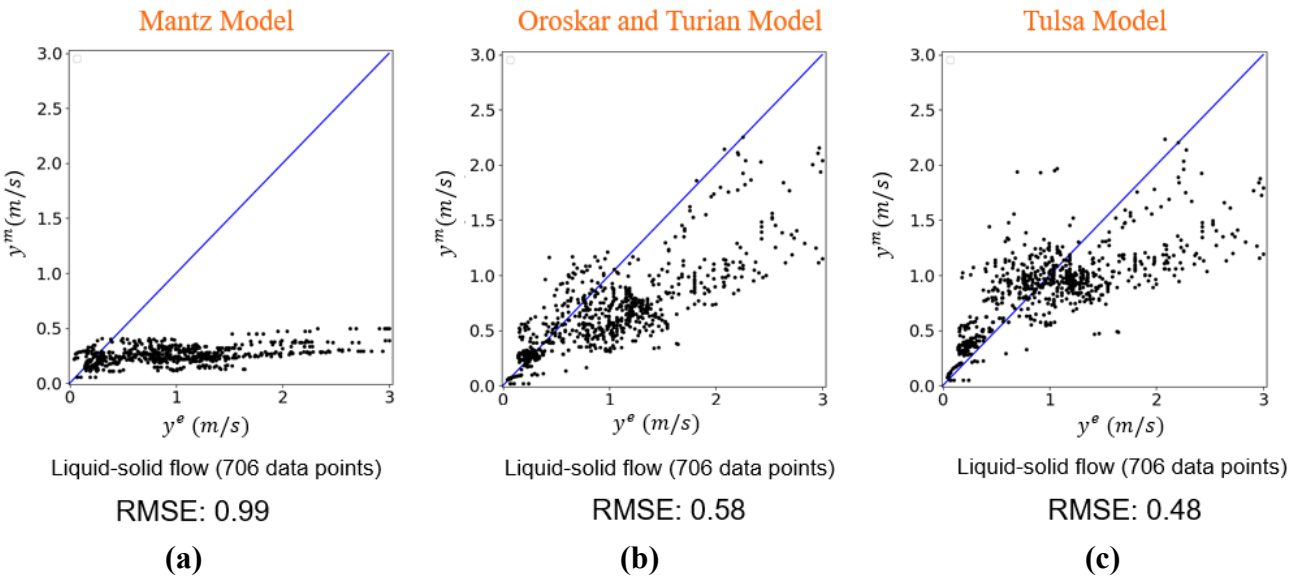

Fig. 12. Semi-mechanistic model predictions of critical velocity for 706 data points. **(a)** Predictions made by the Mantz model, **(b)** Predictions made by the Oroskar and Turian model, **(c)** Predictions made by the Tulsa model.

3.2. Performance of the Hybrid Modeling Framework I

The hybrid model predictions made by framework I are given in Fig. 13. In Fig. 13, the $\hat{y}^e$ values on the y-axis represent the critical velocity predictions made by the hybrid models, the y^e values on the x-axis represent the critical velocity measurements for these data points. The grey lines represent the 95% confidence intervals of the hybrid model predictions. The lowest RMSE and AM values are obtained by the Oroskar and Turian model's predictions.

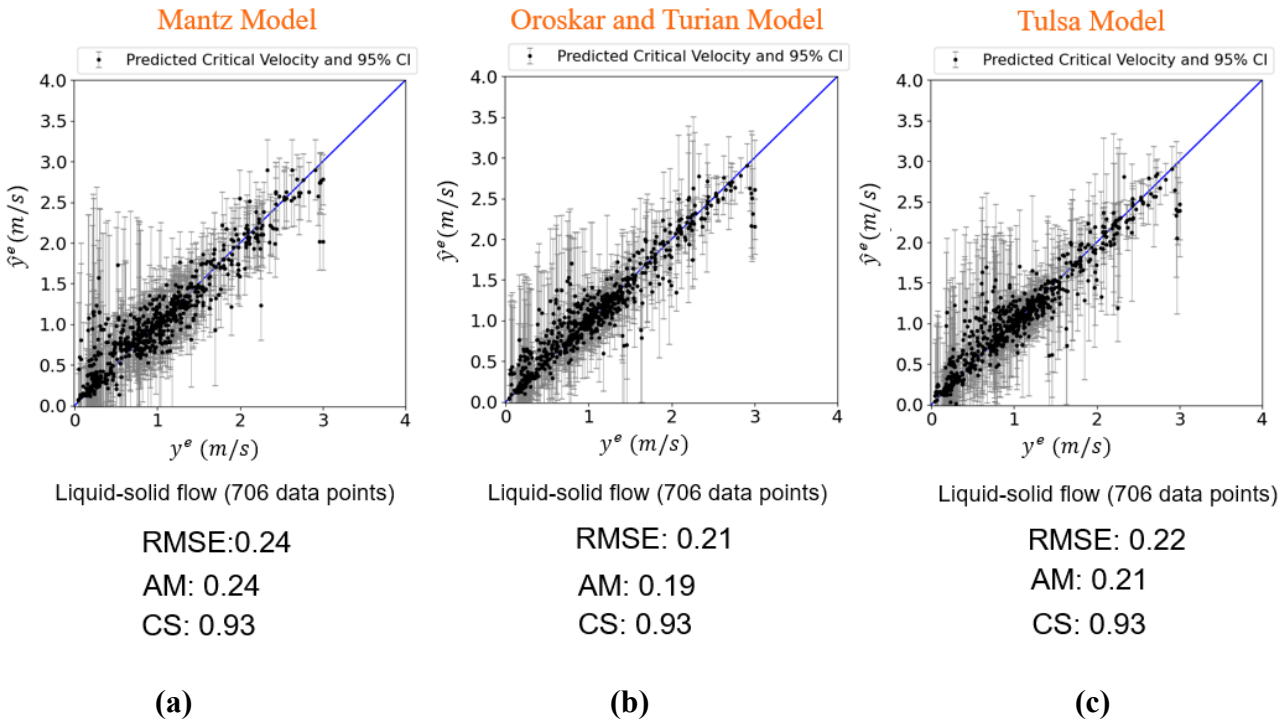

Fig. 13. Hybrid model predictions of critical velocity and their uncertainty where the semi-mechanistic models used are Mantz model (a), Oroskar and Turian model (b), and Tulsa model (c).

A side-by-side comparison of the critical velocity predictions made by the semi-mechanistic models and the corresponding hybrid models is given in Fig. 14 (a) for the Mantz model, Fig. 14 (b) for the Oroskar and Turian model and Fig. 14 (c) for the Tulsa model. With the hybrid modeling

approach, the RMSE values are decreased from 0.99 to 0.24 for the Mantz model, from 0.58 to 0.21 for the Oroskar and Turian model, and from 0.48 to 0.22 for the Tulsa model. For the three hybrid models, it can be observed that the predictions made by the hybrid models are significantly closer to the parity line compared to the semi-mechanistic models' predictions.

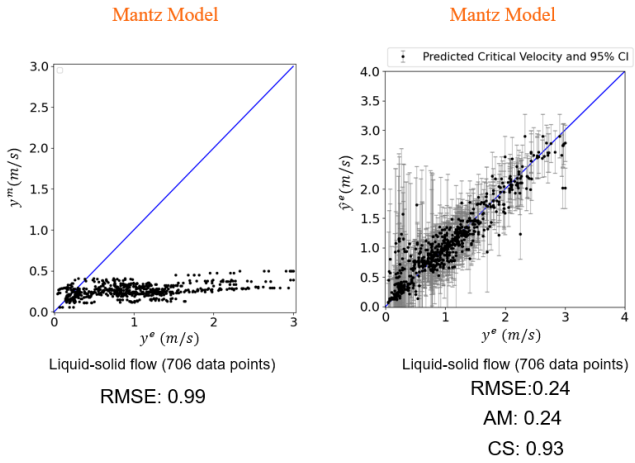

(a)

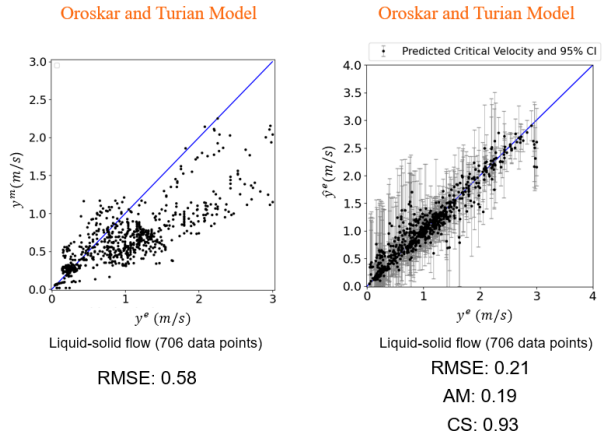

(b)

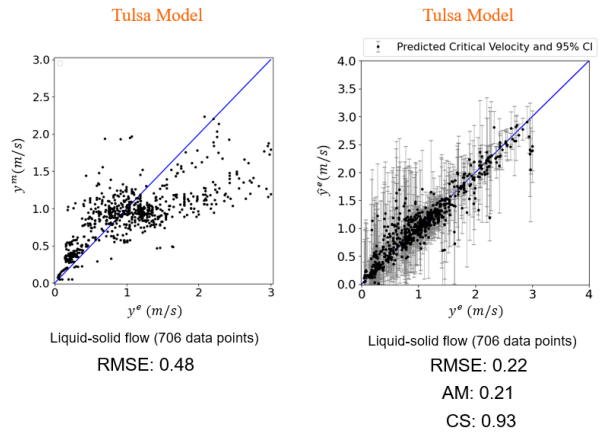

(c)

Fig. 14. Predictions made by the semi-mechanistic models and the corresponding hybrid models. (**a)** Predictions made by the Mantz model and the corresponding hybrid model, (**b)** by the Oroskar and Turian model and the corresponding hybrid model, **(c)** by the Tulsa model and the corresponding hybrid model.

For the 706 data points, the range of experimental measurements of the critical velocity is from ~0 to ~3 m/s approximately which can be seen in the x-axis of the sub figures in Fig.14. These experimental velocity measurements have different ranges of input parameters. Once the predictions made by the semi-mechanistic models are examined in Figs. 11 and 12, the predictions are better for certain ranges of experimental velocity measurements with different input parameter ranges. For example, the Mantz model (Fig. 12 (a)) predictions agree with experimentally measured velocities within the range of ~0 to ~1 m/s approximately. The data points in this range typically have low solid concentrations, and the Mantz model was developed for critical velocity predictions at low solid concentrations. Since the Mantz model doesn't include the solid concentration term in its model equation, it is not able to capture the effect of increasing solid concentrations in its predictions.

A high variance in experimental velocity measurements is observed in Fig. 13, which corresponds to certain ranges of input parameters. The solid transport models have been developed using different assumptions, which makes some models more appropriate for predicting critical velocity in certain operating conditions and others not appropriate. This makes it challenging to select a *"universal"* semi-mechanistic model that is applicable to a wide range of operating conditions. Although hybrid models correct the predictions of the selected semi-mechanistic models, some variance remains. We hypothesize that using the correct semi-mechanistic models will improve predictions with hybrid models. Hybrid Modeling Framework 2 is developed to study this hypothesis. The next section discusses the labeling structure for the dataset and the performance of classifier models used in the model selection process of the Hybrid Modeling Framework 2.

3.3. Results and Discussion of Hybrid Modeling II Framework

3.3.1. Labeling Structure

We employed Bland-Altman (BA) plots to illustrate pairwise comparisons of the critical velocity predictions made by three semi-mechanistic models. Fig. 15 shows the pairwise comparison of critical velocity predictions of the three semi-mechanistic models using the BA plots. The primary purpose of BA plots is to observe the distribution of differences and categorize the dataset into two groups based on the similarity or dissimilarity of predictions made by two models (Altman and Bland, 1983). The x-axis in a BA plot can be any variable. For our analysis, we utilized the volumetric sand concentration as the x-axis because it is a crucial input variable that influences the predictions of the semi-mechanistic models. The y-axis for the BA plots is the modified percent differences between the two semi-mechanistic model predictions, as defined in Equations 21 to 23 (Section 2.3.1). For instance, in Fig. 15 (a), we observe how the predictions made by the Mantz model compare to those of the Oroskar and Turian models as the concentration changes. It is evident that these two models diverge in their predictions with increasing concentration. This observation aligns with our understanding of the models; the Mantz model does not adequately capture the effects of concentration, particularly at high levels, since the concentration term is not included in its model equation.

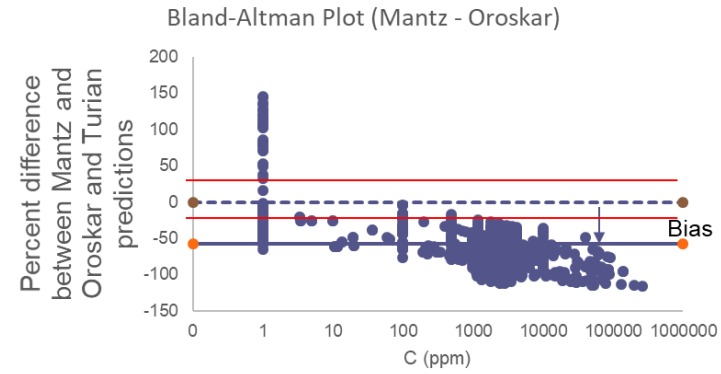

(a)

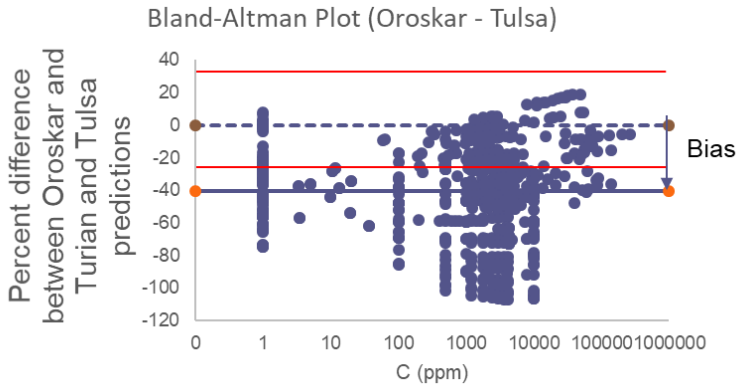

(b)

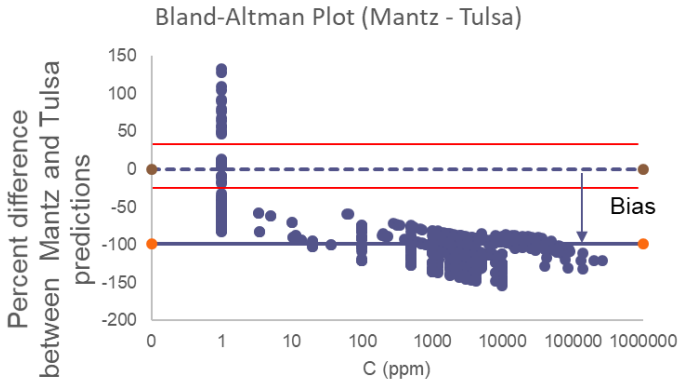

(c)

Fig. 15. BA Plots show the percent difference of the predictions made by Mantz and Oroskar and Turian (a), Oroskar and Turian and Tulsa (b), and Mantz and Tulsa (c) models on the y-axis versus volumetric concentration on the x-axis for two-by-two comparison of the models.

We use the mean and standard deviation of the percentage difference in predictions between the two models (as shown on the y-axis of the figures in Fig. 15) to group our data points. Employing an 80% confidence interval (CI), yields agreement limits of +30% and -30% on the y-axis (indicated by the red lines in Fig. 15). It is assumed that the predictions of the models are similar for data points falling within the agreement limits, i.e., within the red lines and that the predictions of the two models are dissimilar for data points that are outside of the agreement limits. After extracting similar and dissimilar data points from BA Plots, the experimental data set is divided and labeled into six distinct groups (Section 2.3.1), and the final data groups are shown in Fig. 16.

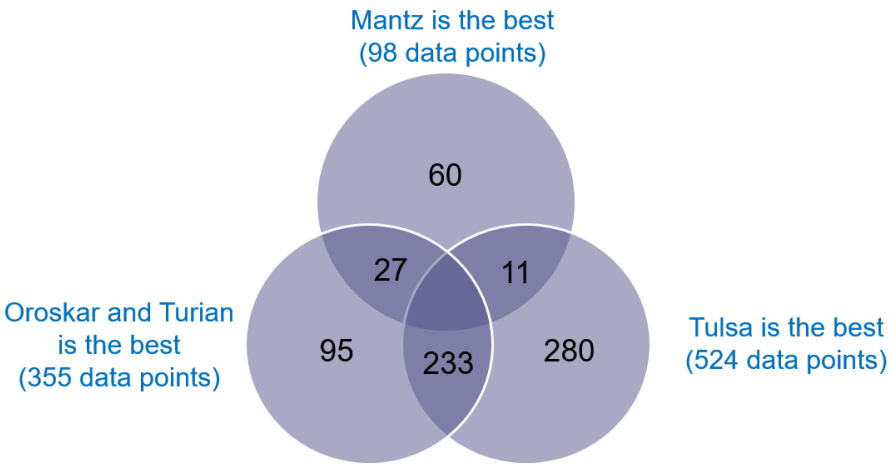

Fig. 16. Vann diagram for labeled data set.

There are 98 data points labeled "Use Mantz model," 355 labeled "Use Oroskar and Turian model," and 524 labeled "Use Tulsa model," which correspond to the best predictions made by these models. It is important to note that the total number of labeled data points does not equal the overall total of 706 data points. This discrepancy arises from the labeling structure used, which allows data points to be assigned to multiple labels if their predictions are equally good. For instance, there are 233 data points that fall within the intersection of the Oroskar and Turian, and the Tulsa

models. This means that for these data points, both the Oroskar and Turian, and the Tulsa models provide equally good predictions, and thus, these points are included in both labels.

The labeled data points are used to train three classifier models. For instance, the Mantz model is trained with a dataset that includes 98 data points labeled “Use Mantz model” and 608 data points labeled “Do not use Mantz model.” The other two classifier models are trained in a similar manner. The Oroskar and Turian model is trained with 355 data points labeled “Use Oroskar and Turian model” and 351 data points labeled “Do not use Oroskar and Turian model.” Finally, the Tulsa model is trained with 524 data points labeled “Use Tulsa model” and 182 data points labeled “Do not use Tulsa model.”

The Tulsa Model, with the highest number of labeled data points, is considered the best model, as it is more representative of the entire experimental data set. In contrast, the Mantz Model has the fewest labeled data points; these data points correspond to experimentally measured velocities in the approximate range of 0 to 1 m/s, as shown in Fig. 21 (a). This limitation arises because the Mantz Model does not account for the effect of volumetric concentration in its equations, and the 98 labeled data points exhibit low volumetric concentration values. Consequently, using the Mantz Model for conditions with high volumetric concentration is not advisable. Through this labeling structure, we also observed that certain models are unsuitable for specific operating conditions.

This observation underscores the importance of accurately selecting semi-mechanistic models for new operating conditions. The next section discusses the performance of these classifier models.

3.3.2. Performance of the classifier models used for semi-mechanistic model selection process in the Hybrid Modeling Framework II

The three different classifier models are built using three different machine-learning algorithms. Mantz model classifier, Oroskar and Turian model classifier, and Tulsa model classifier are built with Random Forest (RF), Gaussian Process Classifier (GPC), and Support Vector Machine (SVM) algorithms. The performances of these models can be found in the following sections.

Random Forest Results

The "number of estimators" which correspond to the number of trees in the forest and the "max features" which correspond to the number of features that are considered for each split, are used as hyperparameters for the random forest algorithm. The optimal hyperparameters are found through a grid search strategy with cross-validation and given in Table 2.

Table 2. Optimal hyperparameters for the Random Forest.

Hyperparameters	**Mantz Model**	**Oroskar and Turian Model**	**Tulsa Model**
Number of estimators	100	250	100
Max Features	6	2	1

The hyperparameters are used in the training of the models, and the performances of these models are tested on the test data set, which corresponds to 10% of the total number of data points (706 data points). Figure 17 presents the confusion matrices for three classifier models utilizing the

Random Forest algorithm. The ratio of labels for the two classes is maintained consistently in both the training and test datasets. The confusion matrices reveal that the Mantz and Tulsa models exhibit relatively unbalanced datasets, while the Oroskar and Turian models demonstrate a balanced dataset. Additionally, we can observe the number of data points associated with each label in the test dataset, as well as how many of these labels are correctly predicted by the classifier models. The evaluation metrics, precision, recall, F1 score, MCC score, and accuracy can be seen in Tables 3, 4, and 5 for the Mantz Model, Oroskar and Turian Model and Tulsa Model classifiers, respectively. Since perfect classifiers would yield metric values of 1, the results in these tables indicate that the Random Forest model performs well across the three classifier models.

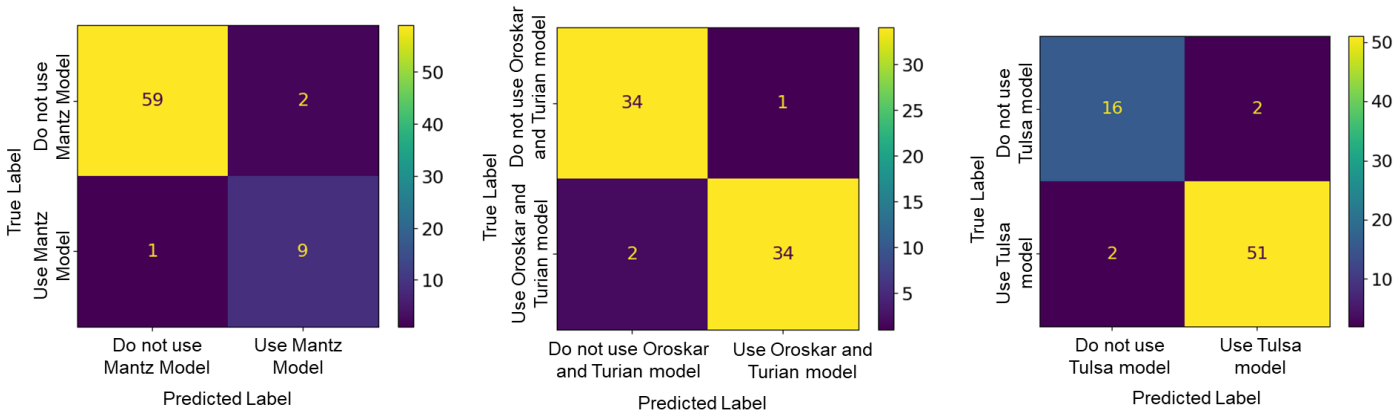

Fig. 17. The confusion matrixes for the three classifier models by the Random Forest.

Table 3. The classification report for the Mantz Model Classifier by the Random Forest.

Mantz Classifier	**Precision**	**Recall**	**F1 Score**	**MCC**	**Accuracy**
Do not use Mantz model	0.98	0.97	0.98	0.83	95.7%
Use Mantz Model	0.82	0.90	0.86		

Table 4. The classification report for the Oroskar and Turian Model Classifier by the Random Forest.

Oroskar and Turian Classifier	**Precision**	**Recall**	**F1 Score**	**MCC**	**Accuracy**
Do not use Oroskar and Turian model	0.94	0.97	0.96	0.92	95.7%
Use Oroskar and Turian model	0.97	0.94	0.96		

Table 5. The classification report for the Tulsa Model Classifier by the Random Forest.

Tulsa Classifier	**Precision**	**Recall**	**F1 Score**	**MCC**	**Accuracy**
Do not use Tulsa model	0.89	0.89	0.89	0.85	94.4%
Use Tulsa model	0.96	0.96	0.96		

GPC Results

The kernel type in the Gaussian Process Classifier algorithm is used as the only hyperparameter. Among five different kernels, the optimal kernels are found as ‘polynomial’ for the Mantz model and ‘exponential’ for the Oroskar and Turian, and Tulsa models.

Table 6. Optimal hyperparameters for Gaussian Process Classifier.

Hyperparameters	**Mantz Model**	**Oroskar and Turian Model**	**Tulsa Model**
Kernel	Poly	Exponential	Exponential

The confusion matrices regarding the GPC for three classifier models are given in Fig. 18 which shows the number of data points for the true labels and the correctly predicted labels for the two classes. Classification reports can be seen in Tables 7, 8, and 9 for the Mantz Model, Oroskar and Turian Model, and Tulsa Model classifiers, respectively. Since perfect classifiers would yield metric values of 1, the results in these tables indicate that the Gaussian Process Classifier model performs well across the three classifier models.

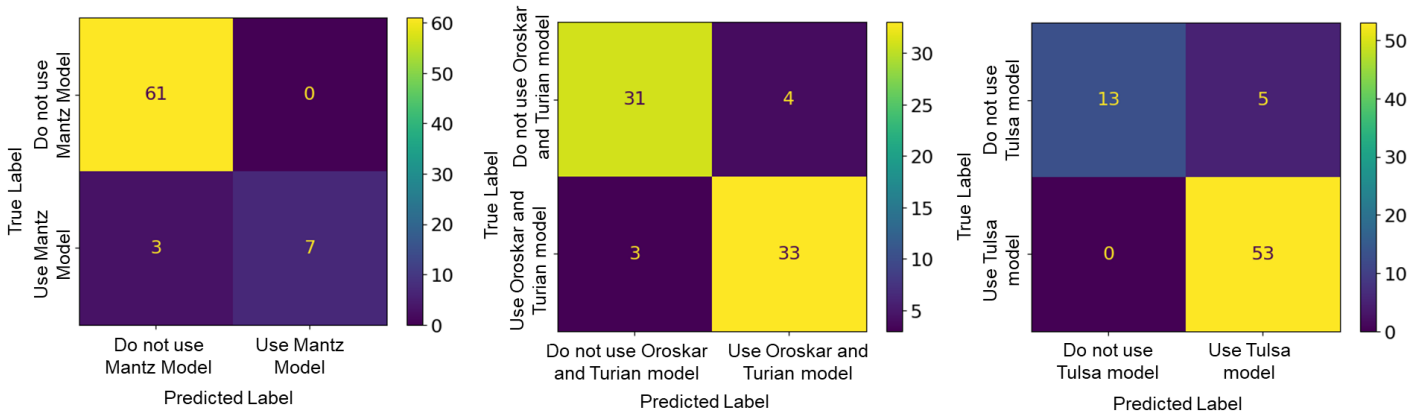

Fig. 18. The confusion matrixes for the three classifier models by the Gaussian Model Classifier.

Table 7. The classification report for the Mantz Model Classifier by the GPC.

Mantz Classifier	**Precision**	**Recall**	**F1 Score**	**MCC**	**Accuracy**
Do not use Mantz model	0.95	1.00	0.98	0.82	95.7%
Use Mantz model	1.00	0.70	0.82		

Table 8. The classification report for the Oroskar and Turian Model Classifier by the GPC.

Oroskar and Turian Classifier	**Precision**	**Recall**	**F1 Score**	**MCC**	**Accuracy**
Do not use Oroskar and Turian model	0.91	0.89	0.90	0.80	90.1%
Use Oroskar and Turian model	0.89	0.92	0.90		

Table 9. The classification report for the Tulsa Model Classifier by the GPC.

Tulsa Classifier	**Precision**	**Recall**	**F1 Score**	**MCC**	**Accuracy**
Do not use Tulsa model	1.00	0.72	0.84	0.81	93%
Use Tulsa model	0.91	1.00	0.95		

SVM Results

The hyperparameters of 'C', 'Gamma', and 'kernel' used in Support Vector Machines algorithm are optimized and found through grid search strategy with cross-validation and the optimal values of them are given in Table 10. The 'rbf' kernel and the 'gamma' values of 10 were chosen for all three classifier models. Since the 'C' parameter is inversely related to the margin size between the hyperplanes, it can be said that the Mantz and Tulsa model classifier models have smaller margins between two classes compared to the Oroskar and Turian Model which is potentially related to the distribution of the imbalanced data set for the Mantz and Tulsa models.

Table 10. Optimal hyper parameters for Support Vector Machines.

Hyper parameters	**Mantz Model**	**Oroskar and Turian Model**	**Tulsa Model**
C	1000	10	1000
Gamma	10	10	10
Kernel	rbf	rbf	rbf

The confusion matrices are given in Fig. 19 for the SVM algorithm that is used for three classifier models. The evaluation metrics that are found through confusion matrices are given in Tables 11, 12, and 13 respectively for three classifier models. Since perfect classifiers would yield metric values of 1, the results in these tables indicate that the Support Vector Machines model performs well across the three classifier models.

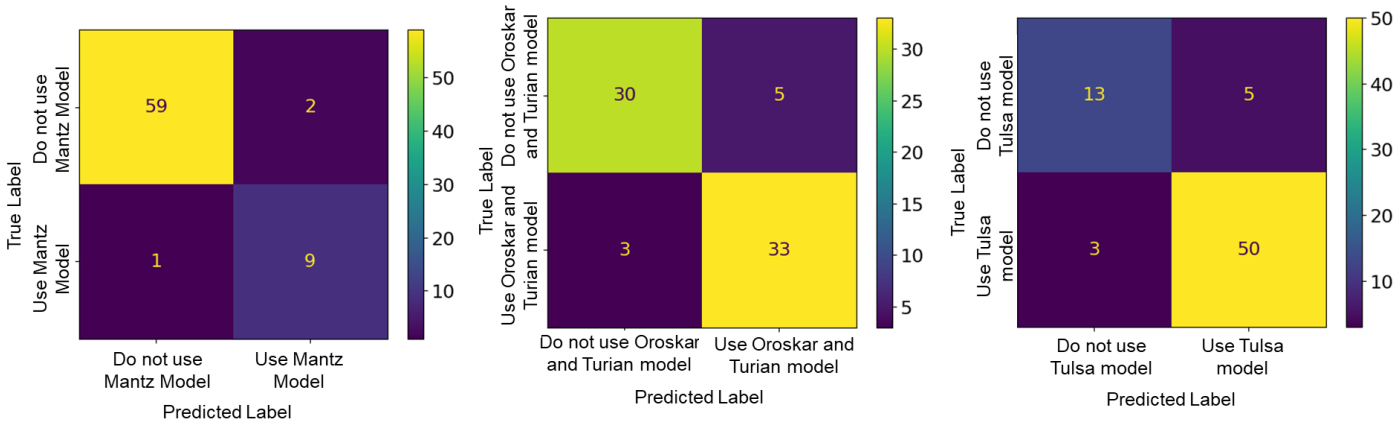

Fig. 19. The confusion matrixes for the three classifier models by the Support Vector Machines.

Table 11. The classification report for the Mantz Model Classifier by the SVM.

Mantz Classifier	**Precision**	**Recall**	**F1 Score**	**MCC**	**Accuracy**
Do not use Mantz model	0.98	0.97	0.98	0.83	95.7%
Use Mantz model	0.82	0.90	0.86		

Table 12. The classification report for the Oroskar and Turian Model Classifier by the SVM.

Oroskar and Turian Classifier	**Precision**	**Recall**	**F1 Score**	**MCC**	**Accuracy**
Do not use Oroskar and Turian model	0.91	0.86	0.88	0.78	88.7%
Use Oroskar and Turian model	0.87	0.92	0.89		

Table 13. The classification report for the Tulsa Model Classifier by the SVM.

Tulsa Classifier	**Precision**	**Recall**	**F1 Score**	**MCC**	**Accuracy**
Do not use Tulsa model	0.81	0.72	0.76	0.69	88.7%
Use Tulsa model	0.91	0.94	0.93		

One of the important evaluation metrics in the assessment of the best models in this work is the MCC score. The comparison of the MCC scores for the three classifier models using three different algorithms is given in Fig. 20. Overall, the RF algorithm gives the highest MCC score for the three models on average. The second-best algorithm is GPC, and it is followed by the SVM algorithm.

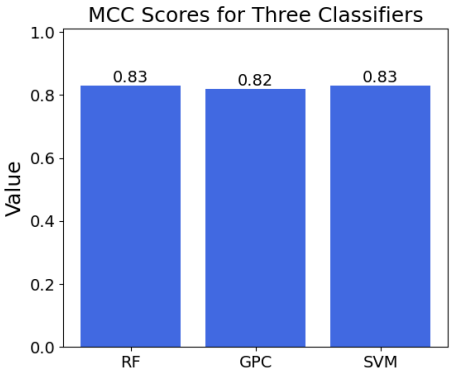

Fig. 20. (a) MCC scores by three classifiers for the Mantz model

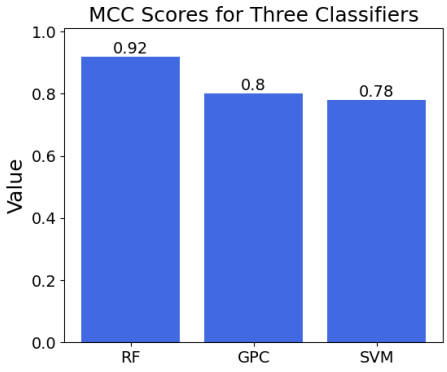

Fig. 20. (b) MCC scores by three classifiers for the Oroskar and Turian model

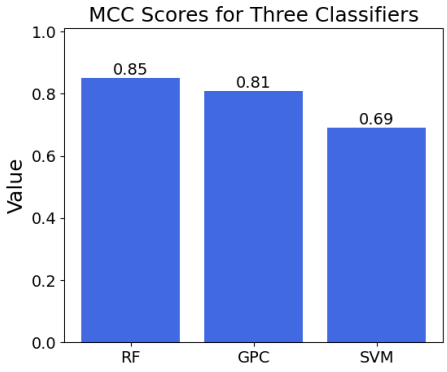

Fig. 20. (c) MCC scores by three classifiers for the Tulsa model

Fig. 20. MCC scores by three classifiers for the three semi-mechanistic models.

We developed three different classifier models using three algorithms, all of which demonstrated good performance. Among these, the Random Forest algorithm yielded the best results across all evaluation metrics considered in this work.

3.4. Performance of the Hybrid Modeling Framework II

This section presents the results of the Hybrid Modeling Framework II, detailing the predictions made by both the semi-mechanistic models and the corresponding hybrid models for the labeled data set. In Fig. 21, the graphs on the left illustrate the critical velocity predictions from the semi-mechanistic models, while the graphs on the right show the predictions from the hybrid models, which are trained using the labeled data set.

Comparing the predictions of the semi-mechanistic models with those of the hybrid models reveals that the hybrid models yield more accurate results (Fig. 21). The root mean square error (RMSE) values decrease from 0.13 to 0.09 for the Mantz model, from 0.6 to 0.16 for the Oroskar and Turian model, and from 0.51 to 0.21 for the Tulsa model. In Figs. 21 (a), (b), and (c), AM values of as 0.07, 0.18 and 0.20 and CS values of 0.95, 0.93, 0.93 are obtained respectively for the hybrid models in which the lowest AM value and highest CS is obtained by the hybrid model that uses Mantz model as the semi-mechanistic model. Overall, the predictions from the hybrid models align more closely with the parity line than those from the semi-mechanistic models.

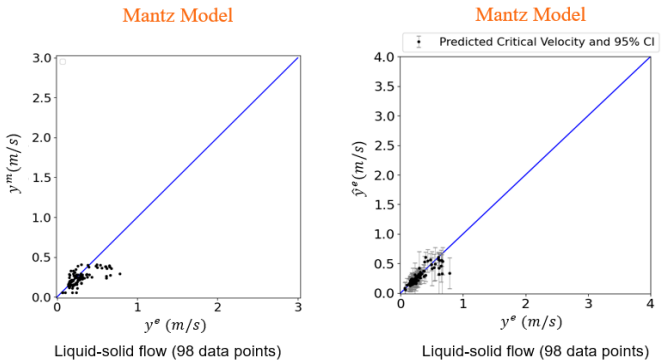

Liquid-solid flow (98 data points)

RMSE: 0.13

Liquid-solid flow (98 data points)

RMSE: 0.09
AM: 0.07
CS: 0.95

(a)

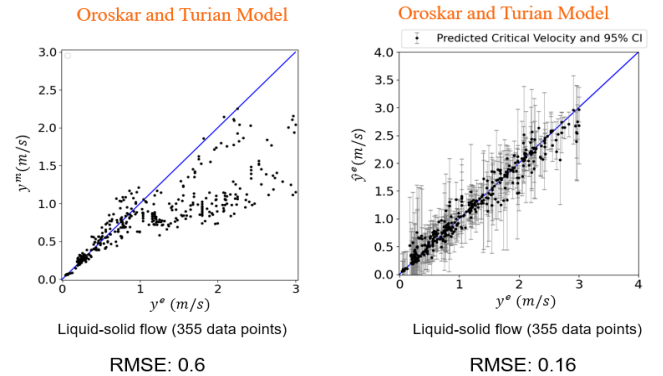

Liquid-solid flow (355 data points)

RMSE: 0.6

Liquid-solid flow (355 data points)

RMSE: 0.16
AM: 0.18
CS: 0.93

(b)

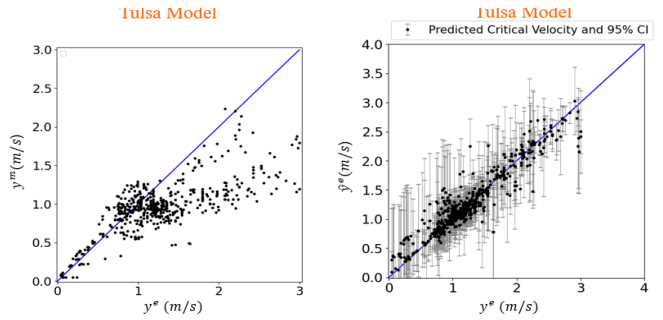

Liquid-solid flow (524 data points)

RMSE: 0.51

Liquid-solid flow (524 data points)

RMSE: 0.21
AM: 0.20
CS: 0.93

(c)

Fig. 21. Predictions made by the semi-mechanistic models and the corresponding hybrid models. (**a**) Predictions made by the Mantz model and the corresponding hybrid model, (**b**) by the Oroskar and Turian model and the corresponding hybrid model, **(c)** by the Tulsa model and the corresponding hybrid model.

3.5. Comparison of the two hybrid modeling frameworks

Figures 22, 23, and 24 compare predictions from two hybrid modeling frameworks using Mantz, Oroskar and Turian, and Tulsa semi-mechanistic models. The left figures show predictions by Hybrid Modeling Framework I, while the right figures show predictions by Hybrid Modeling Framework II. Both hybrid modeling frameworks utilize a parallel structure in their approach. The main distinction between the hybrid models generated by Hybrid Modeling Framework II and those from Framework I is that the former's Gaussian Process Models (GPM) are trained using labeled data and are integrated into the semi-mechanistic model selection process. This means that the preferred semi-mechanistic model among the three will be paired with its corresponding hybrid model, which is trained with the labeled dataset specific to that model. For instance, if the Mantz model is recommended as the semi-mechanistic model for a particular operating condition, the hybrid model from Hybrid Modeling Framework II will be employed. This hybrid model's data-driven components are trained with the model discrepancy values from the 'Use Mantz model' labeled dataset. Overall, the hybrid models produced by Hybrid Modeling Framework II are anticipated to provide more accurate predictions than those generated by Hybrid Modeling Framework I.

In Fig. 22, a comparison of hybrid modeling frameworks is presented using the Mantz model as the semi-mechanistic model. Figs. 22 (a) and 22 (b) illustrate the predictions made by the Mantz model for both the entire dataset and the labeled dataset (denoted as 'Use Mantz model'), alongside the corresponding experimental measurements. The RMSE calculated by the Mantz model for the overall data set (0.99) is higher than the corresponding RMSE for the labeled data set (0.13) which indicates that the Mantz model gives more accurate predictions for the labeled data set. Figs. 22 (c) and 22 (d) show the predictions from the hybrid models utilizing Hybrid Modeling Frameworks

I and II, respectively, in comparison to the experimental measurements. This analysis reveals that Hybrid Modeling Framework II predictions yield smaller RMSE and AM values compared to Framework I. Additionally, the width of the predicted uncertainty is narrower in Fig. 22 (d) than in Fig. 22 (c). Comparing Fig. 22 (a) with Fig. 22 (c) and Fig. 22 (b) with Fig. 22 (d) clearly illustrates that both hybrid modeling frameworks enhance the predictions made by the semi-mechanistic models. The RMSE values decreased from 0.13 to 0.09 for Hybrid Modeling Framework II and from 0.99 to 0.24 for Hybrid Modeling Framework I.

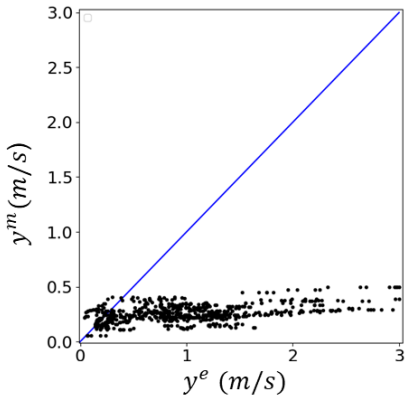

Fig. 22. (a) Mantz model velocity predictions for the whole data set vs. Experimental velocities

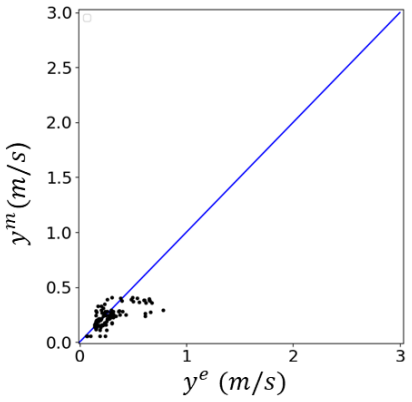

Fig. 22. (b) Mantz model velocity predictions for the labeled data set vs. experimental velocities

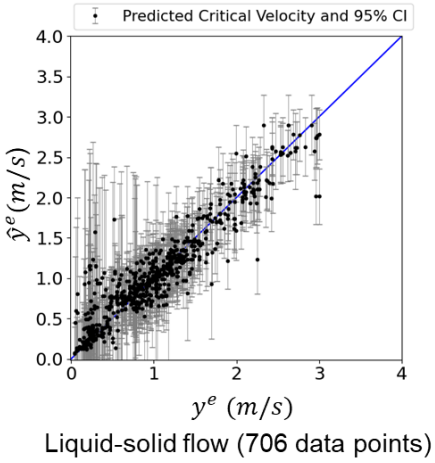

Fig. 22. (c) Hybrid model (trained with the whole data set) velocity predictions for the whole data set vs. experimental velocities

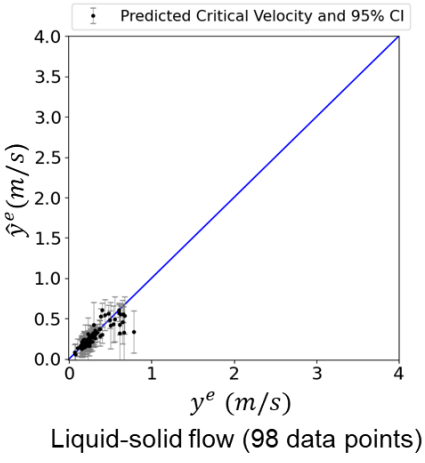

Fig. 22. (d) Hybrid model (trained with the labeled data set) velocity predictions for the labeled data set vs. experimental velocities

Fig. 22. Comparison of the predictions by the hybrid modeling frameworks for the Mantz model being the semi-mechanistic model.

In Fig. 23, the hybrid modeling frameworks comparison where Oroskar and Turian are used as the semi-mechanistic model can be seen. Fig. 23. (a) and Fig. 23. (b) shows the predictions made by the Oroskar and Turian critical velocity predictions versus the experimental measurements for the whole data set and the labeled data set (as 'Use Oroskar and Turian model') respectively. The RMSE value in Fig. 23. (b) is slightly higher than the RMSE value in Fig. 23. (a) although Fig. 23. (b). shows the predictions for the labeled data set. This is because labeling is done in a way that data points are grouped so that certain models have the best predictions out of the three semi-mechanistic models studied. For example, for some data points that are labeled as 'Use Oroskar and Turian model' doesn't necessarily mean that these predictions are good. It means that for those data points, the Oroskar and Turian model gave the best predictions compared to Mantz and Tulsa models. Or it might also mean that the Oroskar and Turian predictions are equally good with either the Mantz model or Tulsa model predictions.

Comparison of Fig. 23. (a) & Fig. 23. (c) and Fig. 23. (b) & Fig. 23. (d) shows that two hybrid modeling frameworks improve the predictions made by the semi-mechanistic models and the RMSE values are decreased from 0.6 to 0.16 for the Hybrid Modeling Framework II, and from 0.58 to 0.21 for the Hybrid Modeling Framework I. This comparison reveals that the decrease in the RMSE and AM values is greater for the Hybrid Modeling Framework II (from 0.6 to 0.16) even though the RMSE value in Fig. 23. (b) is slightly higher than the RMSE value of Fig. 23. (a).

Additionally, once the predictions on Fig. 23. (c) & Fig. 23. (d) is compared, the predictions on Fig. 23. (d) are closer to the parity line and the width of the predicted uncertainty for these predictions is relatively lower which shows that more accurate predictions are obtained by the Hybrid Modeling Framework II, compared to Hybrid Modeling Framework I.

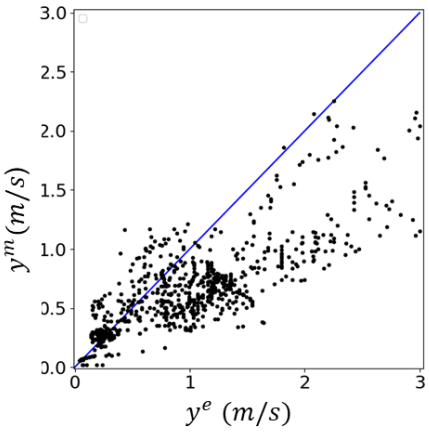

Fig. 23. (a) Oroskar and Turian model velocity predictions for the whole data set vs. experimental velocities

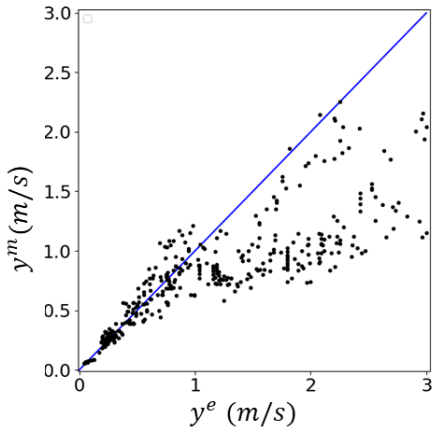

Fig. 23. (b) Oroskar and Turian model velocity predictions for the labeled data set vs. experimental velocities

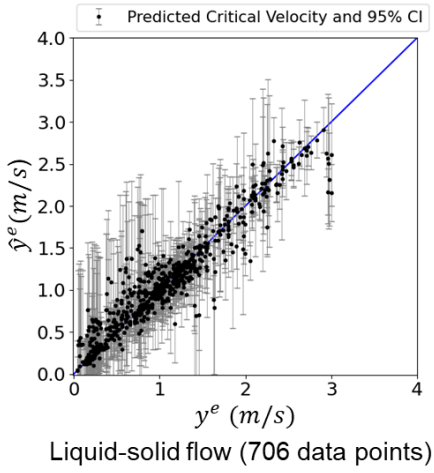

Fig. 23. (c) Hybrid model (trained with the whole data set) velocity predictions for the whole data set vs. experimental velocities

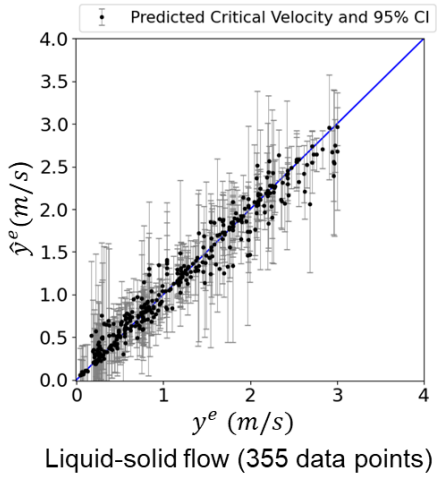

Fig. 23. (d) Hybrid model (trained with the labeled data set) velocity predictions for the labeled data set vs. experimental velocities

Fig 23. Comparison of the predictions by the hybrid modeling frameworks for the Oroskar and Turian model being the semi-mechanistic model.

In Fig. 24, the hybrid modeling frameworks comparison where the Tulsa model is used as the semi-mechanistic model can be seen. Fig. 24. (a) and Fig. 24. (b) show the predictions made by the Tulsa model predictions versus the experimental measurements of critical velocity for the whole data set and the labeled data set (as 'Use Tulsa model') respectively. The RMSE value on Fig. 24. (b) is slightly greater than the one on Fig. 24. (a). This is because these labeled data sets represent the predictions that either the Tulsa model is best or the other two models are equally best together with the Tulsa model.

Comparison of Fig. 24. (a) & Fig. 24. (c) and Fig. 24. (b) & Fig. 24. (d) shows that two hybrid modeling frameworks improve the predictions made by the semi-mechanistic models and the RMSE values are decreased from 0.51 to 0.21 for the Hybrid Modeling Framework II, and from 0.48 to 0.22 for the Hybrid Modeling Framework I. It can be observed that more accurate predictions are made by the Hybrid Modeling Framework II compared to Hybrid Modeling Framework I because a greater decrease in RMSE (from 0.51 to 0.21) is obtained for the Hybrid Modeling Framework II. However, this accuracy is not much compared to the hybrid models that use the Mantz, and Oroskar and Turian models because the RMSE and AM values in Fig. 24. (c) and Fig. 24. (d) is quite close to each other.

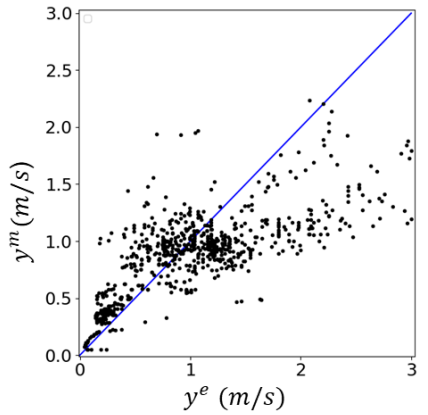

Fig. 24. (a) Tulsa model velocity predictions for the whole data set vs. experimental velocities

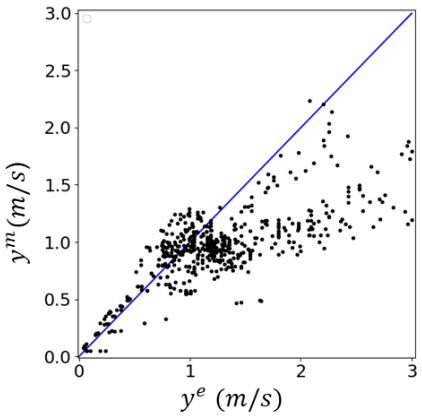

Fig. 24. (b) Tulsa model velocity predictions for the labeled data set vs. experimental velocities

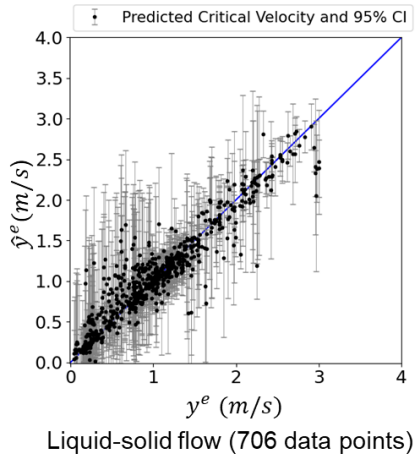

Fig. 24. (c) Hybrid model (trained with the whole data set) velocity predictions for the whole data set vs. experimental velocities

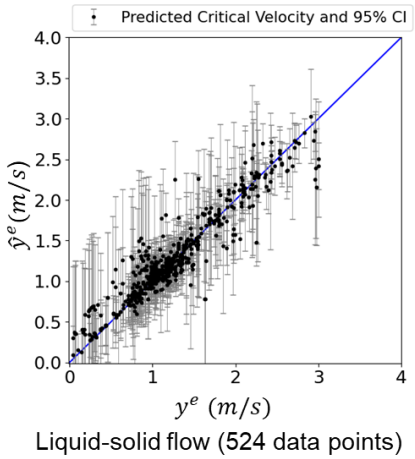

Fig. 24. (d) Hybrid model (trained with the labeled data set) velocity predictions for the labeled data set vs. experimental velocities

Fig. 24. Comparison of the predictions by the hybrid modeling frameworks for the Tulsa model being the semi-mechanistic model.

Another comparison is performed to compare the accuracy of velocity predictions made by the two different hybrid modeling frameworks. The classifier model performances are shown in Section 3.3.2. The confusion matrices of three classifier models are given to show the performances of these models. Considering all the metrics to assess the performances of classifier models, Random Forest is chosen as the best-performing model to be used in the model selection process. For this new comparison of Hybrid Modeling Framework I and II, the predictions for the True Positive (TP) values in Fig.17. are investigated. The data points on that confusion matrix represent the test data set (10% of the whole data set) and these are the data points that the model has not seen before (not used in the model training). True Positives (TP) values in Fig.17. represents the 9, 34, and 51 data points that their labels are 'Use Mantz model', 'Use Oroskar and Turian model', and 'Use Tulsa model' respectively and their labels are correctly predicted by the classifier models. The predictions for these 9, 34, and 51 data points made by the semi-mechanistic models and two different hybrid modeling frameworks are represented in Figs. 25 to 27.

Fig. 25 shows the predictions of the 9 data points that are correctly labeled as 'Use Mantz model'. While Fig. 25. (a) show the predictions made by the Mantz model, Figs. 25. (b) and (c) show the hybrid model predictions by the Hybrid Modeling Framework II and I respectively. Once the RMSE and AM values in Figs. 25. (a) and (b) are compared, lower RMSE and AM values are obtained for the Hybrid Modeling Framework II. Also, a lower width of predicted uncertainty is obtained by the Hybrid Modeling Framework II compared to the Hybrid Modeling Framework I which shows that more accurate predictions are obtained by the Hybrid Modeling Framework II.

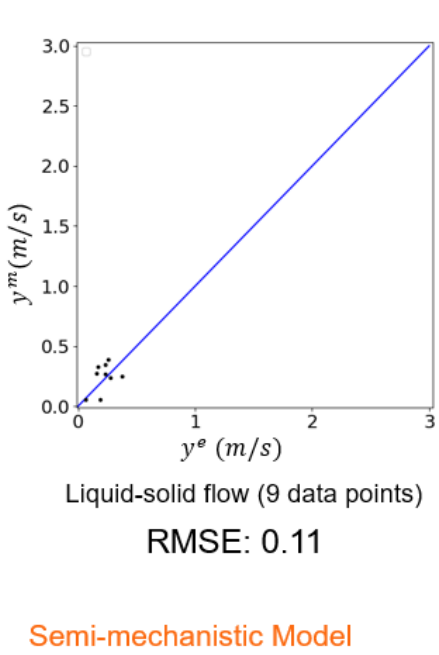

Fig. 25. (a) Mantz model velocity predictions for the TPs in the test data set vs. experimental velocities

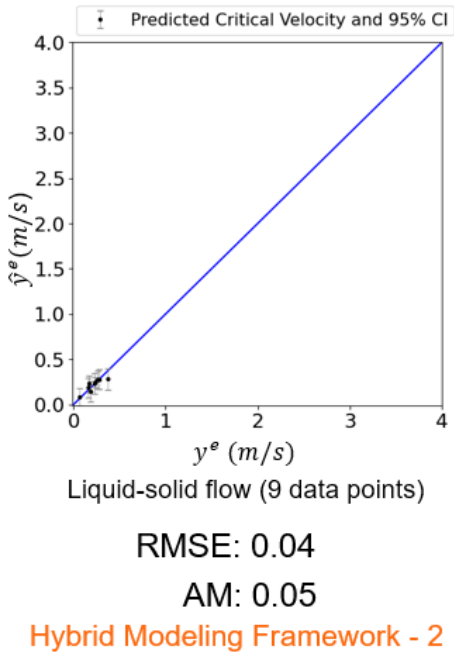

Fig. 25. (b) Hybrid model (trained with the labeled data set) velocity predictions for the TPs in the test data set vs. experimental velocities

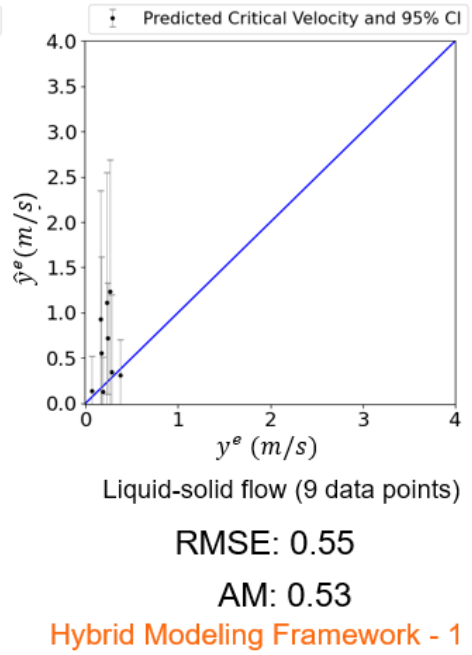

Fig. 25. (c) Hybrid model (trained with the whole data set) velocity predictions for the TPs in the test data set vs. experimental velocities

Fig. 25. Predictions by the Mantz model as the semi-mechanistic model and two corresponding hybrid modeling frameworks for the test data set that are correctly predicted by the Random Forest whose actual label is 'Use Mantz model'.

There are 34 data points that are correctly predicted by the Random Forest model which has the actual labels of 'Use Oroskar Turian model'. The predictions for these data points by the Oroskar and Turian and the corresponding two hybrid models are given in Fig. 26. This comparison reveals that the RMSE is reduced from 0.6 to 0.20 by the Hybrid Modeling Framework I and from 0.6 to 0.13 by the Hybrid Modeling Framework II. This shows that the Hybrid Modeling Framework II provides more accurate predictions of the critical velocity. Comparison of Fig. 26. (b). and Fig. 26.

(c), shows that predictions by Hybrid Modeling Framework II have lower ranges of width of predicted uncertainty.

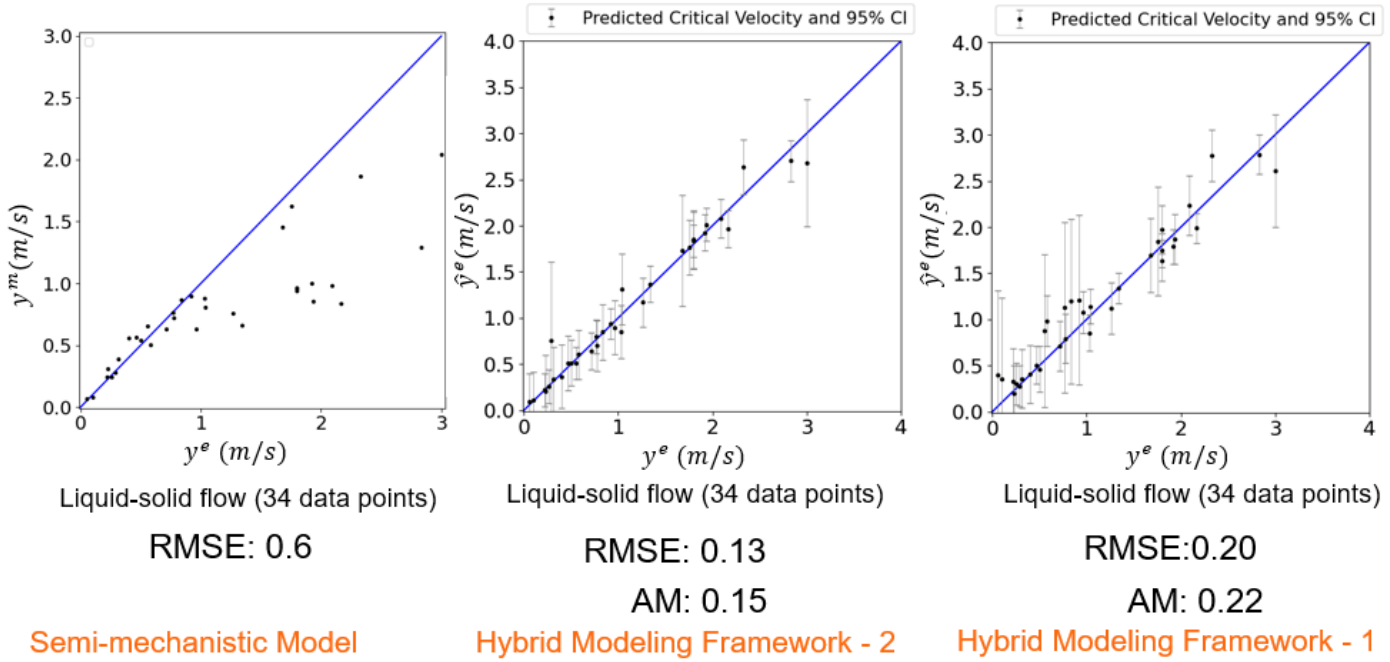

Fig. 26. (a) Oroskar and Turian model velocity predictions for the TPs in the test data set vs. experimental velocities

Fig. 26. (b) Hybrid model (trained with the labeled data set) velocity predictions for the TPs in the test data set vs. experimental velocities

Fig. 26. (c) Hybrid model (trained with the whole data set) velocity predictions for the TPs in the test data set vs. experimental velocities

Fig. 26. Predictions by the Oroskar and Turian model as the semi-mechanistic model and two corresponding hybrid modeling frameworks for the test data set that are correctly predicted by the Random Forest whose actual label is 'Use Oroskar and Turian model'.

The same comparison is given in Fig. 27 for the 54 points that have the label of 'Use Tulsa model' where these data points are correctly predicted by the Random Forest. The RMSE values are decreased from 0.62 to 0.22 by the Hybrid Modeling Framework I and from 0.62 to 0.20 by the Hybrid Modeling Framework II. The RMSE and AM values by the Hybrid Modeling Framework

II are slightly lower than the values by the Hybrid Modeling Framework I. Additionally, there is no considerable difference between the width of predicted uncertainty between the two hybrid modeling frameworks in Fig. 27. (c) and Fig. 27. (d). This suggests that the semi-mechanistic selection process didn't contribute much to the Hybrid Modeling Framework II performance for the Tulsa model. This is because the Tulsa model has the highest number of labeled data points (524 out of 706) compared to the Mantz Oroskar and Turian models and these 524 labeled data points are representative of the whole data set. In other words, for the experimental data set used in this work, the Tulsa model already performs well for the overall data set, and Hybrid Modeling Framework II that has the additional semi-mechanistic model selection process perform slightly better than the Hybrid Modeling Framework I for the Tulsa model.

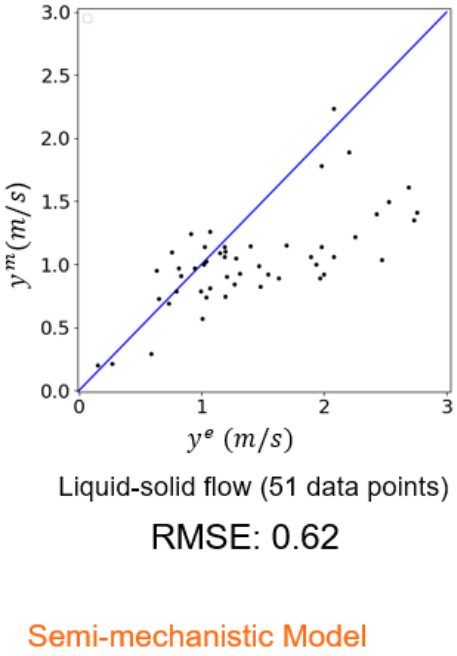

Fig. 27. (a) Tulsa model velocity predictions for the TPs in the test data set vs. experimental velocities

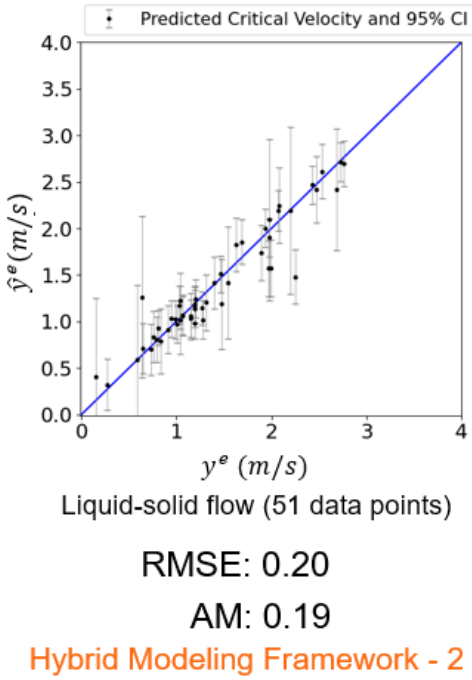

Fig. 27. (b) Hybrid model (trained with the labeled data set) velocity predictions for the TPs in the test data set vs. experimental velocities

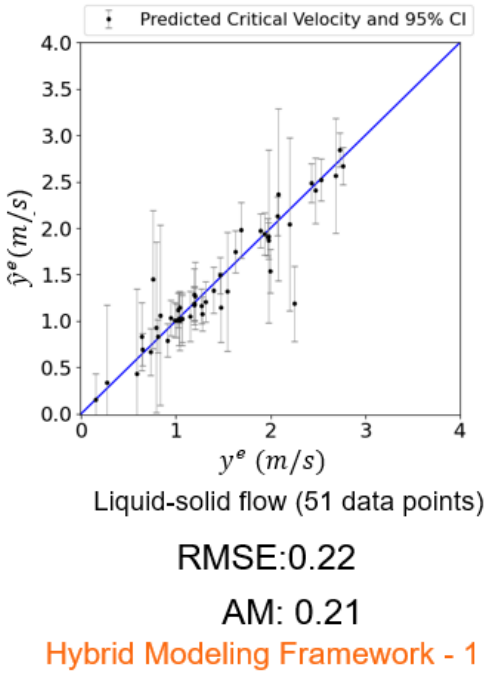

Fig. 27. (c) Hybrid model (trained with the whole data set) velocity predictions for the TPs in the test data set vs. experimental velocities

Fig. 27. Predictions by the Tulsa model as the semi-mechanistic model and two corresponding hybrid modeling frameworks for the test data set that are correctly predicted by the Random Forest whose actual label is 'Use Tulsa model'.

CHAPTER 4 – CONCLUSIONS AND FUTURE DIRECTIONS

In this work, a parallel structure hybrid modeling approach that combines a semi-mechanistic model and a data-driven model is developed to make accurate predictions of critical velocity for solid transport. While the Mantz, Oroskar and Turian, and Tulsa models are used as the semi-mechanistic models, the GPM (Gaussian Process Modeling) is used as the data-driven model. This hybrid modeling structure is referred to as 'Hybrid Modeling Framework I' and a second hybrid modeling framework, namely 'Hybrid Modeling Framework II' that includes an additional semi-mechanistic model selection process is built to make more accurate predictions of critical velocity. Through this semi-mechanistic model selection process, a labeling structure is introduced to label the experimental data set that certain models have the best predictions in which these labeled data set is used later in the training of classifier models that would reveal which semi-mechanistic model to use for a certain operating condition. Random Forest (RF), Support Vector Machines (SVM), and Gaussian Process Classifier (GPC) are used to build 'Mantz Model Classifier', 'Oroskar and Turian Model Classifier', and 'Tulsa Model Classifier'. The MCC scores for the RF, GPC and SVM are in the range of 0.83-0.92, 0.80-0.82 and 0.69-0.83, respectively. The Random Forest outperforms among the studied classifier models.

This overall comparison of critical velocity predictions yields that the hybrid models by the two different hybrid modeling frameworks always outperform the semi-mechanistic models considering the RMSE comparison. Hybrid models by the two different hybrid modeling frameworks always yield lower values of RMSE compared to the semi-mechanistic models. Additionally, these hybrid models also provide prediction uncertainty estimates which cannot be provided by the semi-mechanistic models. Also, hybrid models provide more accurate predictions of critical velocities than semi-mechanistic models overall. Comparison of the RMSE and AM

values by the hybrid models produced by the two different hybrid modeling frameworks reveals that lower RMSE and AM values were obtained by the 'Hybrid Modeling Framework II' compared to 'Hybrid Modeling Framework I'. This shows that velocity predictions are improved further, and more accurate critical velocity estimates are obtained by the 'Hybrid Modeling Framework II'. The overall contribution of using semi-mechanistic model selection in 'Hybrid Modeling Framework II' is observed the most for the Mantz model. A greater decrease in the RMSE and AM values is obtained by the 'Hybrid Modeling Framework II' for the Mantz model compared to the Oroskar and Turian and Tulsa models. The comparison of Hybrid Modeling Frameworks I and II yields that the lowest improvement is observed for the Tulsa model by the Hybrid Modeling Framework II'.

For this work, one future goal would be to expand both the experimental data set, and the number of solid transport models included in the semi-mechanistic model selection process. Also, a wider range of solid transport models can be covered and used for making more accurate predictions of critical velocity. Additional data-driven models can be also used in the hybrid modeling structure and their performances can be assessed to see whether they perform better than the current data-driven model or not. In addition to increasing the number of semi-mechanistic models in the semi-mechanistic model selection process, the proposed labeling structure can be modified in a way that the condition of assigning every data point in the experimental data to at least a model can be removed.

REFERENCES

Agudo, J.R., Dasilva, S., Wierschem, A., 2014. How do neighbors affect incipient particle motion in laminar shear flow? Physics of Fluids 26. https://doi.org/10.1063/1.4874604

Agudo, J.R., Wierschem, A., 2012. Incipient motion of a single particle on regular substrates in laminar shear flow. Physics of Fluids 24. https://doi.org/10.1063/1.4753941

Altman, D.G., Bland, J.M., 1983. Measurement in Medicine: The Analysis of Method Comparison Studies, Source: Journal of the Royal Statistical Society. Series D (The Statistician).

Arevalo, B.G., 2010. Experimental Investigation of Critical Velocities for Sand Transport in Horizontal Single and Two-Phase Flows at Low Sand Concentrations and Comparisons with Existing Models. The University of Tulsa, Tulsa, OK.

Bohling, B., 2009. Measurements of threshold values for incipient motion of sediment particles with two different erosion devices. Journal of Marine Systems 75, 330–335. https://doi.org/10.1016/j.jmarsys.2007.01.014

Bradley, W., Kim, J., Kilwein, Z., Blakely, L., Eydenberg, M., Jalvin, J., Laird, C., Boukouvala, F., 2022. Perspectives on the integration between first-principles and data-driven modeling. Comput Chem Eng. https://doi.org/10.1016/j.compchemeng.2022.107898

Craven, J.P., 1951. A Study of the Transportation of Sand in Pipes. State University of Iowa, Iowa City.

Cremaschi, S., Sarica, C., Subramani, H.J., Soepyan, F.B., Kouba, G.E., 2013. Quantification and Reduction of Uncertainties for Solids Transport Velocity Predictions at Low Concentrations in Near-Horizontal Flow, in: All Days. OTC. https://doi.org/10.4043/24102-MS

Dabirian, R., Mohan, R., Shoham, O., Kouba, G., 2016. Critical sand deposition velocity for gas-liquid stratified flow in horizontal pipes. J Nat Gas Sci Eng 33, 527–537. https://doi.org/10.1016/j.jngse.2016.05.008

De, A.G., Matthews, G., Nickson, T., Fujii, K., Boukouvalas, A., León-Villagrá, P., Ghahramani, Z., Hensman, J., 2017. GPflow: A Gaussian Process Library using TensorFlow Mark van der Wilk, Journal of Machine Learning Research.

Delavan, M., 2012. A Comparison of Experimental Models to Literature Data and Effects of Viscosity in Sand Transportation. The University of Tulsa, Tulsa, OK.

Deng, Y., Avila, C., Gao, H., Mantilla, I., Eden, M.R., Cremaschi, S., 2022. A hybrid modeling approach to estimate liquid entrainment fraction and its uncertainty. Comput Chem Eng 162. https://doi.org/10.1016/j.compchemeng.2022.107796

Ebden, M., 2015. Gaussian Processes: A Quick Introduction.

Géron, A., 2023. Hands-on machine learning with Scikit-Learn, Keras and TensorFlow : concepts, tools, and techniques to build intelligent systems. O'Reilly Media, Inc.

Giavarina, D., 2015. Understanding Bland Altman analysis. Biochem Med (Zagreb) 25, 141–151. https://doi.org/10.11613/BM.2015.015

Goedde E., 1978. To the Critical Velocity of Heterogeneous Hydraulic Transport.

Graf WH, Robinson MP, Yucel O, 1970. Critical Velocity for Solid-Liquid Mixtures. Bethlehem, PA.

Grass, A.J., 1971. Closure to “Initial Instability of Fine Bed Sand.” Journal of the Hydraulics Division 97, 1751–1754. https://doi.org/10.1061/JYCEAJ.0003117

Hayden, J.W., Stelson, T.E., 1971. HYDRAULIC CONVEYANCE OF SOLIDS IN PIPES, in: Advances in Solid–Liquid Flow in Pipes and Its Application. Elsevier, pp. 149–163. https://doi.org/10.1016/B978-0-08-015767-2.50012-0

Hill AL, 2011. Determining the Critical Flow Rates for Low-Concentration Sand Transport in Two-Phase Pipe Flow by Experimentation and Modeling. The University of Tulsa, Tulsa, OK.

IRAJ ZANDI (Ed.), 1971. Advances in Solid–Liquid Flow in Pipes and its Application. Elsevier. https://doi.org/10.1016/C2013-0-02346-8

James, G., Witten, D., Hastie, T., Tibshirani, R., Taylor, J., 2023. An Introduction to Statistical Learning.

Kenchington JM., 1976. Prediction of Critical Conditions for Pipeline Flow of Settling Particles in a Heavy Medium.

Kökpınar, M.A., Göğüş, M., 2001. Critical Flow Velocity in Slurry Transporting Horizontal Pipelines. Journal of Hydraulic Engineering 127, 763–771. https://doi.org/10.1061/(ASCE)0733-9429(2001)127:9(763)

LOBKOVSKY, A.E., ORPE, A. V., MOLLOY, R., KUDROLLI, A., ROTHMAN, D.H., 2008. Erosion of a granular bed driven by laminar fluid flow. J Fluid Mech 605, 47–58. https://doi.org/10.1017/S0022112008001389

Mantz, P.A., 1977. Incipient Transport of Fine Grains and Flakes by Fluids — Extended Shields Diagram. Journal of the Hydraulics Division 103, 601–615. https://doi.org/10.1061/JYCEAJ.0004766

Najmi, K., 2015. PARTICLE TRANSPORT IN SINGLE-PHASE AND MULTIPHASE HORIZONTAL PIPES WITH EMPHASIS ON THE EFFECT OF VISCOSITY.

Obaseki, M., Elijah, P.T., Alfred, P.B., 2022. Development of model to eliminate sand trapping in horizontal fluid pipelines. Journal of King Saud University - Engineering Sciences 34, 425–434. https://doi.org/10.1016/j.jksues.2020.11.006

Oroskar, A.R., Turian, R.M., 1980. The critical velocity in pipeline flow of slurries. AIChE Journal 26, 550–558. https://doi.org/10.1002/aic.690260405

Patankar, N.A., Joseph, D.D., Wang, J., Barree, R.D., Conway, M., Asadi, M., 2002. Power law correlations for sediment transport in pressure driven channel flows. International Journal of Multiphase Flow 28, 1269–1292. https://doi.org/10.1016/S0301-9322(02)00030-7

Ramadan, A., Skalle, P., Johansen, S.T., 2003. A mechanistic model to determine the critical flow velocity required to initiate the movement of spherical bed particles in inclined channels. Chem Eng Sci 58, 2153–2163. https://doi.org/10.1016/S0009-2509(03)00061-7

Rasmussen, C.E., n.d. Gaussian Processes in Machine Learning.

Rasmussen, C.Edward., Williams, C.K.I., 2006. Gaussian processes for machine learning. MIT Press.

Sansana, J., Joswiak, M.N., Castillo, I., Wang, Z., Rendall, R., Chiang, L.H., Reis, M.S., 2021. Recent trends on hybrid modeling for Industry 4.0. Comput Chem Eng. https://doi.org/10.1016/j.compchemeng.2021.107365

Santhamoorthy, P.Z., Williams, B., Sambath, K., Subramani, H.J., Cremaschi, S., 2024. An integrated framework for sand handling in wellbore and surface facilities. Geoenergy Science and Engineering 239. https://doi.org/10.1016/j.geoen.2024.212947

Soepyan, B.F., Cremaschi, S., Sarica, C., Subramani, H.J., 2012. Selection of the Optimal Critical Velocity for Sand Transport at Low Concentrations for Near-Horizontal Flow, in: All Days. OTC. https://doi.org/10.4043/23075-MS

Soepyan, F.B., Cremaschi, S., Sarica, C., Subramani, H.J., Kouba, G.E., 2014. Solids transport models comparison and fine-tuning for horizontal, low concentration flow in single-phase carrier fluid. AIChE Journal 60, 76–122. https://doi.org/10.1002/aic.14255

Stevenson, P., Thorpe, R.B., 2002. Velocity of isolated particles along a pipe in stratified gas–liquid flow. AIChE Journal 48, 963–969. https://doi.org/10.1002/aic.690480506

von Stosch, M., Oliveira, R., Peres, J., Feyo de Azevedo, S., 2014. Hybrid semi-parametric modeling in process systems engineering: Past, present and future. Comput Chem Eng 60, 86–101. https://doi.org/10.1016/j.compchemeng.2013.08.008

Wang, J., 2020. An Intuitive Tutorial to Gaussian Process Regression. https://doi.org/10.1109/MCSE.2023.3342149

WHITE, S.J., 1970. Plane Bed Thresholds of Fine Grained Sediments. Nature 228, 152–153. https://doi.org/10.1038/228152a0

Wicks, M., 1971. TRANSPORT OF SOLIDS AT LOW CONCENTRATION IN HORIZONTAL PIPES, in: Advances in Solid–Liquid Flow in Pipes and Its Application. Elsevier, pp. 101–124. https://doi.org/10.1016/B978-0-08-015767-2.50010-7

Zenz, F.A., 1964. Conveyability of Materials of Mixed Particle Size. Industrial & Engineering Chemistry Fundamentals 3, 65–75. https://doi.org/10.1021/i160009a012